

**Bit Error Rate Performance Analysis of an Optical Fiber Communication System
with a Multi-Core Fiber**

by

Md Jahangir Hossain

MASTER OF SCIENCE IN ELECTRICAL, ELECTRONIC AND
COMMUNICATION ENGINEERING



Department of Electrical, Electronic and Communication Engineering
MILITARY INSTITUTE OF SCIENCE AND TECHNOLOGY, MIRPUR
Jan 2016

The thesis titled “**Bit Error Rate Performance Analysis of an Optical Fiber Communication System with a Multi-Core Fiber**” submitted by Md Jahangir Hossain, Student no: 1013160023(F), Session Oct/2013 has been accepted as satisfactory in partial fulfillment of the requirement for the degree of Master of Science in Electrical, Electronic and Communication on 04 Jan, 2016.

BOARD OF EXAMINERS

1. _____
Dr Satya Prasad Majumder
Professor, EEE Dept, BUET
BUET, Dhaka - 1000
Chairman
(Supervisor)

2. _____
Gp Capt Dr Mohammed Hossam-E-Haider, PhD
Professor and Head
EECE Dept, MIST, Mirpur, Dhaka-1216
Member
(Ex-officio)

3. _____
Maj Hussain Md. Abu Nyeem, PhD, EME
EECE Dept, MIST, Mirpur, Dhaka-1216
Member

4. _____
Dr Md Shah Alam
Professor, EEE Dept, BUET
BUET, Dhaka - 1000
Member
(External)

CANDIDATE'S DECLARATION

It is hereby declared that this thesis or any part of it has not been submitted elsewhere for the award of any degree or diploma.

Md Jahangir Hossain

DEDICATED TO MY PARENTS

Acknowledgement

At first, I must express my utmost gratefulness and sincerest thanks to the Almighty ALLAH, the most merciful, the most gracious for giving me the opportunity to complete my research work and the thesis.

This thesis is the most significant accomplishment in my life. I would like to thank my parents for their continuous support, encouragement and sacrifice throughout the period and I will be indebted to them forever for all they have done.

This is my immense pleasure to express my sincere and profound gratitude to my supervisor Dr. Satya Prasad Majumder, professor EEE Dept, BUET for providing me the opportunity to conduct postgraduate research in area of optical fiber communication. I convey my heartfelt and cordial thank to him for his continuous guidance, kind help and encouragement without which this work would never be possible. It is his inspiration, encourage and untiring supervision that have enabled me to finish this work within the stipulated time.

Finally, I would like to extend my sincere thanks to all the faculty members and staffs of EECE department, MIST for their cordial help and assistance during my study period.

Last but not the least, it would be unjust if I don't mention about the contribution of my family members who have always encouraged me and rendered their support to continue my studies and research work.

Abstract

Multicore Fiber (MCF) is found to be a promising candidate to replace Single Mode Fiber (SMF) in order to increase the capacity of an optical fiber link. In this thesis, investigations are carried out to find out the limitations imposed by crosstalk due to coupling between the cores of an MCF on the Bit Error Rate (BER) performance of a MCF optical link. Analysis is carried out for single mode multicore fiber (MCF) to find the electric fields and power induced from one fiber to another for a given structure of a MCF, number of cores, refractive index profile etc. The expressions of the signal power at the output of the different cores of the MCF with excitation to any one of the cores is found out along with the crosstalk. The expression for the crosstalk power due to coupling among the cores is also determined. The analysis is extended to optical MCF link with an optical pre-amplifier followed by direct detection receiver. Finally, the expression for Signal to Crosstalk plus Noise Ratio (SCNR) at the output of the excited fiber core is found. Computations are carried out for signal power of the desired channel and crosstalk power due to other channels. The BER for a given data rate is then determined numerically for different MCF parameters and transmission distance. The optimum system design parameters like coupling co-efficient between cores of MCF, BER, transmission distance, input power range, gain of the optical pre-amplifier etc, is determined for a given data rate. The outcome of this research work will be useful to design fiber optic system with Multi-core single-mode fiber running at BER comparable to multi-mode fiber links. The proposed system may be a potential candidate for future MIMO fiber optic communication system.

TABLE OF CONTENTS

Contents	Page no
Board of Examiners	i
Declaration	ii
Dedication	iii
Acknowledgement	iv
Abstract	v
List of Figures	ix
List of Tables	xii
List of Abbreviations	xiii
List of Symbols	xiv
 Chapter 1: Introduction	
1.1 Introduction	1
1.2 Structure of optical fiber	1
1.3 Optical fiber communication system	2
1.4 Merits of optical fiber communication system	3
1.5 Generations of optical fiber communication system	5
1.6 Types of Optical fiber	7
1.6.1 Mode Profiles	7
1.6.2 Refractive Index Profile	9
1.6.3 Multicore Fiber (MCF)	11
1.6.3.1 Applications of MCF	15
1.6.3.2 Limitations of MCF	15
1.7 Multiplexing Techniques in Optical Communication System	16
1.7.1 Wavelength Division Multiplexing (WDM)	16
1.7.2 Optical Frequency Division Multiplexing (OFDM)	17
1.7.3 Mode Division Multiplexing (MDM)	19
1.7.3.1 Application of MDM	19
1.7.4 Optical Code Division Multiple Access (Optical CDMA)	20
1.8 Previous Works	21
1.9 Objectives of the Thesis	25
1.10 Organization of the Thesis	26

Chapter 2 : Analysis of Optical Link with MCF

2.1	Introduction	27
2.2	System Model	27
2.2.1	Transmitter Block Diagram	28
2.2.2	Block Diagram of Optical Receiver with Optical Pre-amplifier	30
2.3	System Analysis	31
2.3.1	Mode Coupling Theory in a Seven Core MCF	31
2.4	Analytical Derivation of Optical Signal Power and Crosstalk Power of the MCF link without Optical Pre-Amplifier	36
2.5	Analysis of Electrical SCNR: without optical Pre-amplifier	39
2.5.1	Analysis of electrical output signal and Noises of the MCF Link	39
2.6	Bit Error Rate Analysis	40

Chapter 3: Results and Discussion

3.1	Introduction	42
3.2	Performance results without optical Pre-Amplifier	43
3.2.1	Evaluation of SCNR	43
3.2.2	Effect of BER on Transmission Distance	44
3.2.3	Effect of Coupling Co-efficient on SCNR	46
3.2.4	Effect of Coupling Co-efficient on BER	48
3.2.5	Effect of SCNR over BER	50
3.2.6	Effect of Coupling Co-efficient on Power Penalty	52
3.2.7	Effect of input power on transmission distance	53
3.3	Performance results with optical Pre-amplifier	53
3.3.1	Effect of Electrical SCNR on transmission distance	53
3.3.2	Effect of BER on transmission distance	54
3.3.3	Effect of input power on transmission distance	56
3.3.4	Effect of Coupling Co-efficient on SCNR	56
3.3.5	Effect of Coupling Co-efficient on BER	57
3.3.6	Effect of Optical pre-amplifier Gain on SCNR	58
3.3.7	Effect of Optical pre-amplifier Gain on BER	58
3.3.8	Effect of Optical pre-amplifier Gain on transmission distance	59

3.3.9	Comparisons of results of with and without optical pre-amplifier	60
-------	--	----

Chapter 4: Conclusion and Scope of Future Works

4.1	Introduction	61
4.2	Conclusion	61
4.3	Scope of Future Works	62
	References	63

LIST OF FIGURES

- Fig. 1.1 Basic Structure of an Optical Fiber
- Fig. 1.2 A typical optical fiber communication system
- Fig. 1.3 Optical fiber attenuation as a function of wavelength
- Fig. 1.4 Single mode(SM) Fiber Path
- Fig. 1.5 Multi-mode (MM) Fiber Path
- Fig. 1.6 Types of Fiber Optic Cable
- Fig. 1.7 Schematic of a 7-core MCF
- Fig. 1.8 Schematic of a holey MCF
- Fig. 1.9 Different types of Heterogeneous Fiber
- Fig. 1.10 Cross-sectional view of various structures of MCF
- Fig. 1.11 Various Structures of MCF
- Fig. 1.12 Typical WDM Network
- Fig. 1.13 Block diagram of OFDM Modulation and Demodulation
- Fig. 1.14 OFDM Principle
- Fig. 2.1(a) Block diagram of an Optical MIMO Link with MCF without Optical PA
- Fig. 2.1(b) Block diagram of an Optical MIMO Link with MCF with Optical PA
- Fig. 2.2 Transmitter Block Diagram
- Fig. 2.3 Receiver Block Diagram
- Fig. 2.4 Homogeneous 7-core MCF with core radius 'a'
- Fig. 2.5 Coupling dynamics of a 7 core MCF
- Fig. 3.1 Plots of SCNR at the output of a 7 core MCF as a function of distance with input optical power, $P_{in} = -5$ dBm, -8 dBm and -10 dBm and coupling coefficient, $K_c = 0.5$, data rate, $R_b = 2.5$ Gbps
- Fig. 3.2 Plots of SCNR at the output of a 7 core MCF as a function of distance with input optical power, $P_{in} = -5$ dBm, -8 dBm and -10 dBm and coupling coefficient, $K_c = 0.5$, data rate, $R_b = 10$ Gbps
- Fig 3.3(a) Plots of BER at the output of a 7 core MCF as a function of distance with input optical power, $P_{in} = -20$ dBm for three different data rate of $R_b = 1$ Gbps, 2.5 Gbps and 10 Gbps and coupling coefficient, $K_c = 0.5$
- Fig. 3.3(b) Plots of BER at the output of a 7 core MCF as a function of distance with input optical power, $P_{in} = -18$ dBm for three different data rate of $R_b = 1$ Gbps, 2.5 Gbps and 10 Gbps and coupling coefficient, $K_c = 0.5$

- Fig 3.3(c) Plots of BER at the output of a 7 core MCF as a function of distance with input optical power, $P_{in} = -15$ dBm for three different data rate of $R_b = 1$ Gbps, 2.5 Gbps and 10 Gbps and coupling coefficient, $K_c = 0.5$
- Fig. 3.4(a) Plots of SCNR at the output of a 7 core MCF as a function of coupling coefficient of ranges, $K_c = 0.5- 2.5$ with input optical power, $P_{in} = -3$ dB, data rate, $R_b = 1$ Gbps, for two separate distance, $Z= 100$ m and $Z= 1$ km
- Fig. 3.4(b) Plots of SCNR at the output of a 7 core MCF as a function of coupling coefficient of ranges, $K_c = 0.5- 2.5$ with input optical power, $P_{in} = -3$ dB, data rate, $R_b = 2.5$ Gbps, for two separate distance, $Z= 100$ m and $Z= 1$ km
- Fig. 3.4(c) Plots of SCNR at the output of a 7 core MCF as a function of coupling coefficient of ranges, $K_c = 0.5- 2.5$ with input optical power, $P_{in} = -3$ dB, data rate, $R_b = 10$ Gbps, for two separate distance, $Z= 100$ m and $Z= 1$ km
- Fig. 3.5(a) Plots of BER at the output of a 7 core MCF as a function of coupling coefficient of ranges, $K_c = 0.5- 2.5$ with input optical power, $P_{in} = -2$ dBm, data rate, $R_b = 1$ Gbps and for distances of $Z= 100$ m and $Z= 1$ km
- Fig. 3.5(b) Plots of BER at the output of a 7 core MCF as a function of coupling coefficient of ranges, $K_c = 0.5- 2.5$ with input optical power, $P_{in} = -1$ dBm, data rate, $R_b = 2.5$ Gbps and for distances of $Z= 100$ m and $Z= 1$ km
- Fig. 3.5(c) Plots of BER at the output of a 7 core MCF as a function of coupling coefficient of ranges, $K_c = 0.5- 2.5$ with input optical power, $P_{in} = 1$ dBm, data rate, $R_b = 10$ Gbps and for distances of $Z= 100$ m and $Z= 1$ km
- Fig 3.6(a) Plots of BER at the output of a 7 core MCF as a function of SCNR with input optical power, $P_{in} = 4.5$ dBm for data rate, $R_b = 1$ Gbps
- Fig 3.6(b) Plots of BER at the output of a 7 core MCF as a function of SCNR with input optical power, $P_{in} = 6.5$ dBm for data rate, $R_b = 2.5$ Gbps
- Fig. 3.6(c) Plots of BER at the output of a 7 core MCF as a function of SCNR with input optical power, $P_{in} = 9.5$ dBm for data rate, $R_b = 10$ Gbps
- Fig. 3.7 Plots of power penalty(dB) as a function of coupling co-efficient for different data rates and at transmission distance $Z= 1$ Km.
- Fig. 3.8 Plots of transmission distance as a function of input optical power for different data rate.

- Fig. 3.9(a) Plots of SCNR (dB) as a function of link distance with different input optical power, at a data rate of $R_b = 10$ Gbps, $K_c = 0.5$ and $G = 20$ dB
- Fig. 3.9(b) Plots of SCNR (dB) as a function of link distance with different input optical power, at a data rate of $R_b = 10$ Gbps, $K_c = 1.0$ and $G = 20$ dB
- Fig. 10(a) Plots of BER as a function of link distance with different input power, at a data rate of $R_b = 10$ Gbps, $K_c = 0.5$ and $G = 20$ dB
- Fig. 10(b) Plots of BER as a function of link distance with different input power, at a data rate of $R_b = 10$ Gbps, $K_c = 1.0$ and $G = 20$ dB.
- Fig. 3.11 Plots of transmission distance as a function of power input for different data rate and coupling coefficient, $K_c = 0.5$
- Fig. 3.12 Plots of SCNR (dB) as a function of coupling coefficient for different power input, and $G = 20$ dB
- Fig. 3.13 Plots of BER as a function of link distance for different input power, $R_b = 10$ Gbps and $G = 20$ dB
- Fig. 3.14 Plots of SCNR (dB) as a function of link distance for different gain, G level, $R_b = 10$ Gbps, $P_{in} = -5$ dBm and $K_c = 0.5$
- Fig. 3.15 Plots of BER as a function of Transmission distance for different gain, G level, $R_b = 10$ Gbps, $P_{in} = -5$ dB and $K_c = 0.5$.
- Fig. 3.16 Plots of transmission distance as a function of Gain level for different input power, $R_b = 10$ Gbps, $BER = 10^{-9}$ and $K_c = 0.5$.

LIST OF TABLES

		Page No.
Table 1.1	Generations of Optical Fiber Communications	5
Table 1.2	Different transmission windows of Fiber Optic Transmission	6
Table 1.3	Material/ Bandgap/Wavelength	6
Table 3.1	Parameters for Numerical Computations	42

LIST OF ABBREVIATIONS

BER	Bit Error Rate
WDM	Wavelength Division Multiplexing
MCF	Multi Core Fiber
MM	Multi-Mode
SMF	Single Mode Fiber
MMF	Multi-Mode Fiber
FMF	Few Mode Fiber
EMI	Electromagnetic Interference
SDM	Spatial Division Multiplexing
MDM	Mode Division Multiplexing
LD	Laser Diode
LED	Light Emitting Diode
NDSF	Non Dispersion Shifted Fiber
DSF	Dispersion Shifted Fiber
DWDM	Dense Wavelength Division Multiplexing
NZ-DSF	Non Zero Dispersion Shifted Fiber
ASK	Amplitude Shift Keying
ASE	Amplified Spontaneous Emission
MIMO	Multiple Input Multiple Output
HCPS	Hexagonal Close Pack Structure
TPS	Two pitch structure
ORS	One Ring Structure
PCF	Photonic Crystal fiber
OOK	On Off Keying
LASER	Light Amplification by Stimulated Emission of Radiation
ISI	Inter Symbol Interference
SCNR	Signal to Crosstalk plus Noise ratio
EDFA	Erbium Doped Fiber Amplifier

LIST OF SYMBOLS

λ	Wavelength
d	Core diameter
n_1	Core refractive index
n_2	Cladding refractive index
n_{1p}	refractive index of p-th core
p	P-th core
a_p	Radius of p-th core
A_p	Mode Amplitude of p-th core
$C_k=C_{pq}$	Coupling Co-efficient between p-th and q-th core.
$E_p(z)$	Electric field of p-th core along z direction
β_p	Propagation constant of p-th core
P_{sig}	Signal power
P_{CT}	Crosstalk power
P_{ASE}	ASE power
i_t	Thermal Noise Current
i_p	Photo current
i_d	Dark Current
i_{ASE}	ASE Current
n_{sp}	Spontaneous noise
R_d	Receiver Responsivity
R_b	Data rate
P_{in}	Power Input

CHAPTER 1

INTRODUCTION

1.1 Introduction

Optical fiber has emerged as most reliable communication media in today's context. Almost all Bandwidth hungry application and data transfer technology requires a reliable transmission medium like optical fiber for speedy allocation of information. To fulfill the growing bandwidth requirement, various types of multi-core fibers (MCFs) are developed to apply Space Division Multiplexing (SDM) and Mode division Multiplexing (MDM) [1-3]. Almost every month there is a new improvement of bandwidth or other features' update of optical fiber communication.

1.2 Structure of Optical Fiber

Optical fiber is a dielectric waveguide or medium in which information (voice, data or video) is transmitted in the form of light through a glass or plastic fiber. The basic structure of an optical fiber is shown in Fig. 1.1. It consists of a transparent core with a refractive index n_1 surrounded by a transparent cladding of a slightly less refractive index n_2 . The refractive index of cladding is 1% lower than that of core. Typical value of a core refractive index is 1.50 and a cladding refractive index is 1.48.

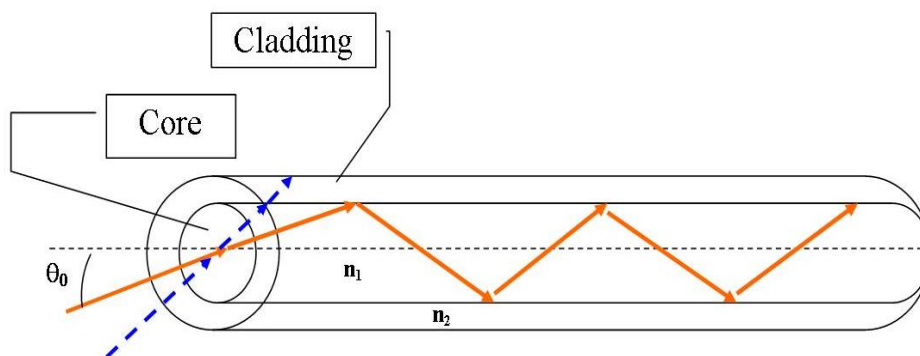


Fig. 1.1 Basic Structure of an Optical Fiber [5]

The cladding supports the waveguide structure, protects the core from absorbing surface contaminants and when adequately thick, substantially reduces the radiation loss to the surrounding air. Glass core fibers tend to have low loss in comparison with plastic core fibers. Additionally, most of the fibers are encapsulated in an elastic, abrasion resistant plastic material which mechanically isolates the fibers from small geometrical

irregularities and distortions. A set of guided electromagnetic waves, also called the modes of the waveguide, can describe the propagation of light along the waveguide. Only a certain number of modes are capable of propagating through the waveguide [4].

1.3 Optical Fiber Communication System

Optical fibers are widely used in communication sectors which permit very efficient transfer of information at higher transmission rate than other transmission media. It is a medium for carrying information from one point to another in the form of light. Due to very low attenuation, less interference, and huge speed, it is used by many telecommunications companies. Currently, almost every telephone conversation, cell phone call, cable television (CATV) signals and Internet data packet are passing through some piece of optical fiber from source to destination.

The process of communication using fiber-optics involves the following basic steps: Creating the optical signal involving the use of a transmitter, relaying the signal along the fiber, ensuring that the signal does not become too distorted or weak, receiving the optical signal, and converting it into an electrical signal.

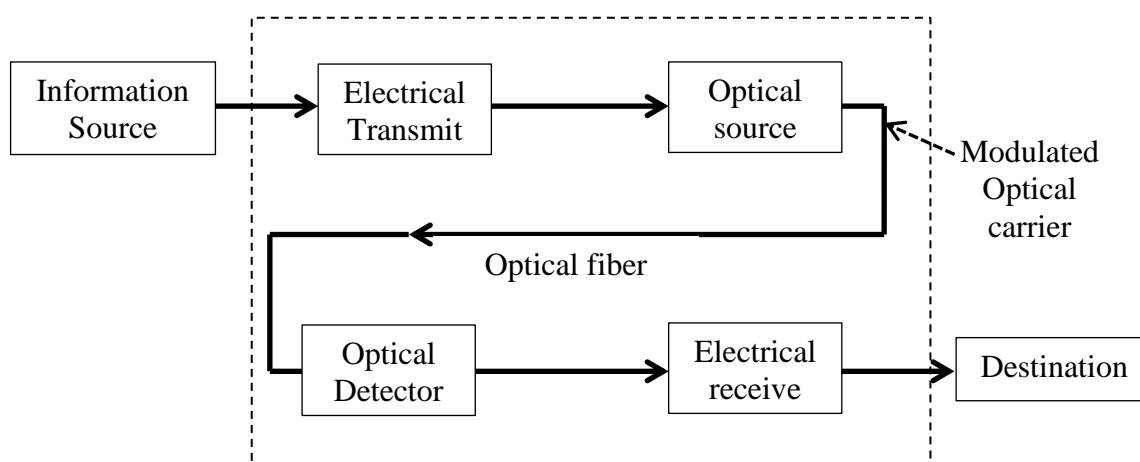


Fig. 1.2 A typical optical fiber communication system [5]

The block diagram of typical optical fiber communication system is shown in Fig. 1.2[5]. The information signal may be voice, data, video etc and the information signal is converted to electrical signal through the transmitter. Here electrical transmitter works as a modulator or multiplexer. In this block diagram, optical source is used. The main function of this optical source is to convert the electrical

signal to optical signal. Laser diode (LD) or light emitting diode (LED) is used as an optical source in optical fiber communication system. They are called optical oscillator. They provide stable, single frequency waves with sufficient power for long distance propagation.

The output of the optical signal pass through the transmission medium and this transmission medium is an optical fiber cable. The optical fiber creates connection between transmitter and receiver. After traveling the desired distance, the optical signal enters to the optical detector and the main functions of this optical detector is to convert optical signal to electrical signal. Semiconductor photodiode is mainly used as an optical receiver.

Detector output contains the transmitted information. These photodetectors are small in size, has low power consumption, has high sensitivity and usually cost effective. Finally, this electrical signal is received by an electrical receiver and convert electrical signal to original signal [6]. For long distance transmission reshaping and amplifying is necessary for getting accurate signal [7]. For that reason optical amplifiers and signal generators are used.

Optical filters, couplers, and switches are used between optical transmitter and optical receiver. The function of a coupler is to combine light into or split light out of a fiber. A splitter is a coupler that divides the optical signal on one fiber to two or more fibers [8]. The weak and distorted signal after detection at the receiver is amplified and restored to original shape by the amplifier.

1.4 Merits of Optical Fiber Communication

Optical fiber has emerged as most reliable communication media. In many applications copper wire is been replaced by Optical fiber due to its certain advantages/merits. Most important merits of optical fiber are enumerated below [5]:

Enormous potential bandwidth: The optical carrier frequency has much greater potential transmission Bandwidth (BW) than metallic cable systems.

Small size and weight: Optical fiber has small diameters. Hence, even when such fibers are covered with protective coating they are far smaller and lighter than the corresponding copper cables.

Electrical Isolation: Optical fibers which are fabricated from glass or sometimes a plastic polymer are electrical insulators and unlike their metallic counterpart, they do not exhibit earth loop or interface problems. This property makes optical fiber transmission ideally suited for communication in electrically hazardous environments as fiber created no arcing or spark hazard at abrasion or short circuits.

Signal security: The light from optical fiber does not radiate significantly and therefore they provide a high degree of signal security. This feature is attractive for military, banking and general data transmission i.e. computer networks application.

Low transmission loss: The technological developments in optical fiber over last twenty years has resulted in optical cables which exhibits very low attenuation or transmission loss in comparison with best copper conductors.

Potential low cost: The glass which provides the optical fiber transmission medium is made from sand. So, in comparison to copper conductors, optical fiber offers the potential for low cost line communication.

Higher carrying capacity - Because optical fibres are thinner than copper wires, more fibres can be bundled into a given-diameter cable than copper wires. This allows more phone lines to go over the same cable or more channels to come through the cable into cable TV box.

Less signal degradation - The loss of signal in optical fibre is less than in copper wire.

Light signals - Unlike electrical signals in copper wires, light signals from one fibre do not interfere with those of other fibres in the same cable. This means clearer phone conversations or TV reception.

Non-flammable - Because no electricity is passed through optical fibres, there is no fire hazard.

Immunity to interference. An especially important feature of optical fibers relates to their dielectric nature. This provides optical waveguides with immunity to electromagnetic interference (EMI), such as inductive pickup from signal-carrying wires and lightning. It also ensures freedom from electromagnetic pulse (EMP) effects, which is of particular interest in military applications.

1.5 Generations of Optical Fiber Communication System

Table 1.1 shows the different generations of optical fiber communication [4]. In generation I, mostly GaAs based LEDs and LDs having emission wavelength 0.8 μm were used. From 1974 to 1978, graded index multimode fibers were used. From 1978 onwards, only single mode fibers are used for long distance communication. During the second generation the operating wavelength is shifted to 1.3 μm to overcome loss and dispersion. Further InGaAsP hetero-junction laser diodes are used as optical sources. In the third generation the operating wavelength is further shifted to 1.55 μm and the dispersion-shifted fibers (DSF) are used. Further single mode direct detection is adopted. In the fourth generation erbium doped optical (fiber) amplifiers (EDFA) are fabricated and the whole transmission and reception are performed only in the optical domain. Wavelength division multiplexing (WDM) is introduced to increase the bit rate. In the proposed next generation (V generation), soliton based lossless and dispersion less optical fiber communication will become a reality. At that time, the data

Table 1.1: Generations of Optical Fiber Communications

Generation	Wavelength of optical source(μm)	Bitrate(Mbps)	Repeater Spacing (Km)	Loss(dB/Km)	Existed Upto
I	0.8	4.5	10	1	1980
II	1.3	1.7×10^2	50	<1	1987
III	1.55	1.0×10^4	70	<0.2	1990
IV	1.55	1.0×10^5	100	<0.002	2000
V	1.55	$>1.0 \times 10^9$	>100	<0.002	

rate may increase beyond 1000 Tb/s. Table 1.2 and table 1.3 shows the different transmission windows of fiber optic communication and material properties (wavelength) of optical fiber respectively [4].

Table 1.2: Different transmission windows of Fiber Optic Transmission

Band	Description	Wavelength range
O band	Original	1260–1360 nm
E band	Extended	1360–1460 nm
S band	Short wavelengths	1460–1530 nm
C band	Conventional (“Erbium window”)	1530–1565 nm
L band	Long wavelengths	1565–1625 nm
U band	Ultra-long wavelengths	1625–1675 nm

Table 1.3: Material/ Bandgap/Wavelength

Material	InP	InAs	GaP	GaAs	AlAs	GaInP	AlGaAs	InGaAs	InGaAsP
Wavelength	0.92	3.6	0.55	0.87	0.59	0.64-0.68	0.8-0.9	1.0-1.3	0.9-1.7

Fig. 1.3 shows three transmission windows of fiber optic communication [7]. It describes the attenuation in dB/km as a function of wavelength (λ).

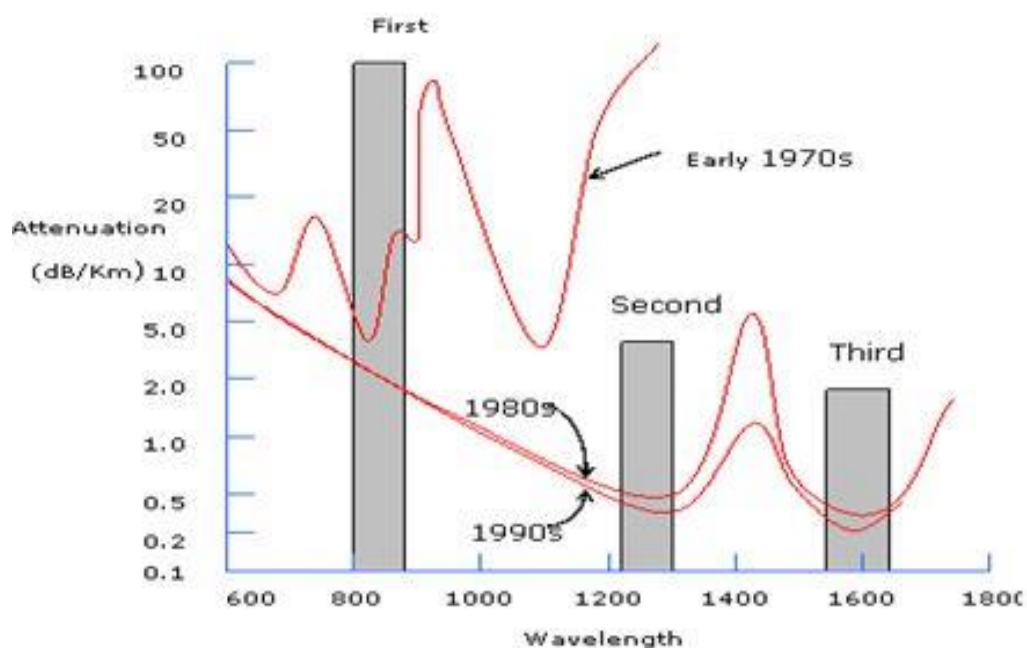


Fig. 1.3 Optical fiber attenuation as a function of wavelength [7]

1.6. Types of Optical Fibers

Optical fiber can be categorized into many types depending on optical field propagation properties (mode), refractive index profile, core structure and configurations etc. Few important types are summarized below [9-10]:

1.6.1 Mode Profiles

Fiber optic can be categorized in two broad categories according to the mode profile:

Single mode/Mono mode and Multimode.

Single mode

In a single mode fiber, the core diameter is reduced to few wavelengths of the incoming light. For example for a beam with $\lambda = 0.55 \mu\text{m}$, the core diameter should be of the order of $4.5 \mu\text{m}$. Under these circumstances, the core is so small that only the primary mode can travel inside the fiber. Single-mode fiber allows for a higher capacity to transmit information because it can retain the fidelity of each light pulse over longer distances, and it exhibits no dispersion caused by multiple modes. Single-mode fiber also enjoys lower fiber attenuation than multimode fiber. Thus, more information can be transmitted per unit of time. Like multimode fiber, early single-mode fiber was generally characterized as step-index fiber meaning the refractive index of the fiber core is a step above that of the cladding rather than graduated as it is in graded-index fiber. Modern single-mode fibers have evolved into more complex designs such as matched clad, depressed clad and other exotic structures.

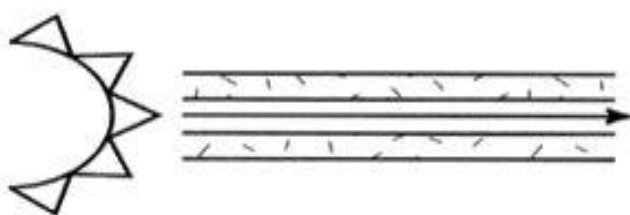


Fig. 1.4 Single mode(SM) Fiber Path

Single-mode fiber has disadvantages as well. The smaller core diameter makes the coupling light into the core more difficult. The tolerances for single-mode connectors and splices are also much more demanding. Single-mode fiber has gone through a continuing evolution for several decades now. As a result, there are three basic classes of single-mode fiber used in modern telecommunications systems. The oldest and most widely deployed type is non dispersion-shifted fiber (NDSF). These fibers were initially

intended for use near 1310 nm. Later, 1550 nm systems made NDSF fiber undesirable due to its very high dispersion at the 1550 nm wavelength. To address this shortcoming, fiber manufacturers developed dispersion-shifted fiber (DSF) that moved the zero-dispersion point to the 1550 nm region. Years later, scientists would discover that while DSF worked extremely well with a single 1550 nm wavelength, it exhibits serious nonlinearities when multiple, closely-spaced wavelengths in the 1550 nm were transmitted in DWDM systems. Recently, to address the problem of nonlinearities, a new class of fibers was introduced. These are classified as non-zero-dispersion-shifted fibers (NZ-DSF). Single-mode fiber gives us a higher transmission rate and up to 50 times more distance than multimode, but it also costs more. Single-mode fiber shrinks the core down so small that the light can only travel in one ray. The typical core size of a single-mode fiber is 9 microns. Since only one mode is allowed to travel down the fiber path, the total internal reflection phenomenon does not occur and the concept of numerical aperture is reduced to its definition (the same as for multimode fibers). Single-mode fibers carry optical signals in the second and third telecom windows where attenuation is minimized. The center wavelength of the laser emitting into the fiber is approximately 1310 nm and 1550 nm, respectively. The attenuation of a single-mode fiber is of about 0.4 dB per km in the second window and 0.25 dB per km in the third window.

Multi-mode

In a multimode fibre, the core diameter is much bigger than the wavelength of the transmitted light. A number of modes can be simultaneously transmitted. The primary mode travels parallel to the axis of the fibre and therefore takes the minimum time to reach the end of the fibre. When the incoming beam enters with an angle respect to the fibre axis, the light will follow a longer path and therefore will take longer to reach the end. The number of modes that can be transmitted along the fibre increases with the core diameter. Multimode fiber is the first to be manufactured and commercialized. Multimode fiber is easier to couple than single-mode optical fiber. Multimode fiber may be categorized as step-index or graded-index fiber. Multimode fiber gives us high bandwidth at high speeds (10 to 100 Mbps - Gigabit at 275 m to 2 km) over medium distances. Light waves are dispersed into numerous paths, or modes, as they travel through the cable's core typically in 850 nm or 1300 nm. Typical multimode fiber core diameters are 50, 62.5, and 100 micrometers. However, in long cable runs (greater than

3000 feet [914.4 meters), multiple paths of light can cause signal distortion at the receiving end, resulting in an unclear and incomplete data transmission. So designers now call for single mode fiber in new applications using Gigabit and beyond.

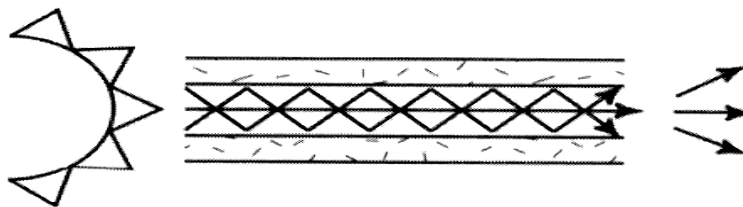


Fig. 1.5 Multi-mode (MM) Fiber Path

Fig. 1.5 shows how the principle of total internal reflection applies to multimode step-index fiber. Because the core's index of refraction is higher than the cladding's index of refraction, the light that enters at less than the critical angle is guided along the fiber. Three different light waves travel down the fiber. One mode travels straight down the center of the core. A second mode travels at a steep angle and bounces back and forth by total internal reflection. The third mode exceeds the critical angle and refracts into the cladding. Intuitively, it can be seen that the second mode travels a longer distance than the first mode, causing the two modes to arrive at separate times. This disparity between arrival times of the different light rays is known as dispersion, and the result is a muddled signal at the receiving end. Multimode fibers used in telecom or data communication applications have a core size of 50 or 62.5 microns. This large core size is responsible for the fiber to support multiple transverse electromagnetic modes for a given frequency and polarization. When light enters the fiber, it naturally scatters and the multiple modes travel simultaneously along the path. Multimode fibers carry optical signals in the first and second telecom windows where the attenuation is minimized. The center wavelength of the laser emitting into the fiber is approximately 850 nm and 1300 nm, respectively. One key characteristic of a multimode fiber is its modal bandwidth. It represents the capacity of a fiber to transmit a certain amount of information and is expressed in MHz*km. The typical attenuation of a multimode fiber is of about 1 to 1.5 decibels (dB) per kilometer (km).

1.6.2 Refractive Index Profile

Step Index fibers have sharp boundaries between the core and cladding, with clearly defined indices of refraction. The entire core uses single index of refraction. Step index

fibers are the most used fibers in fields other than telecommunications. They are relatively cheap and they have the widest range of core diameters: basically from 50 μm up to 2 mm. The material may be plastic, liquid or glass.

Graded Index fibers are widely used in telecommunications; they are inexpensive and easy to procure. Unlike step index fiber, a graded index core contains many layers of glass, each with a lower index of refraction as we go outward from the axis. The effect of this grading is that the light rays are speeded up in the outer layers, to match those rays going the shorter pathway directly down the axis. The result is that a graded index fiber equalizes the propagation times of the various modes so that data can be sent over a much longer distance and at higher rates before light pulses start to overlap and become less distinguishable at the receiver end. Graded index fibers are commercially available with core diameters of 50, 62.5 and 100 microns. Fig. 1.6 shows various types of optical fiber [7]

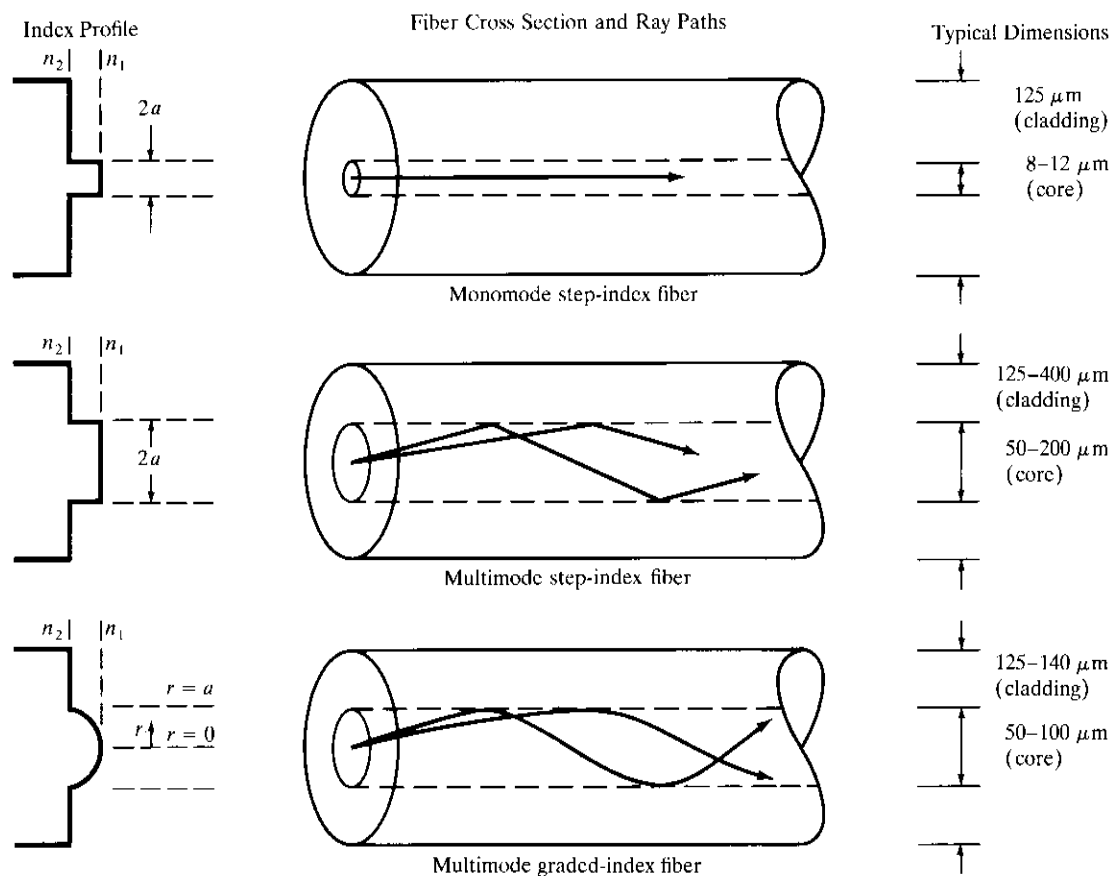


Fig. 1.6 Types of Fiber Optic Cable [7]

Single Mode Step Index Fiber:

Single mode fiber has a core diameter of 8 to 9 microns, which only allows one light path or mode.

Multimode Step-Index Fiber:

Multimode fiber has a core diameter of 50 or 62.5 microns (sometimes even larger). It allows several light paths or modes. This causes modal dispersion – some modes take longer to pass through the fiber than others because they travel a longer distance.

Multimode Graded-Index Fiber

Graded-index refers to the fact that the refractive index of the core gradually decreases farther from the centre of the core. The increased refraction in the centre of the core slows the speed of some light rays, allowing all the light rays to reach the receiving end at approximately the same time, reducing dispersion

1.6.3 Multicore Fiber (MCF)

Multi-Core Fiber (MCF) is a fiber that can have multiple cores inside a single cladding. As their name implies, it provides more light-carrying cores than the SSMF (Standard Single Mode Fiber) to significantly increase the bandwidth capacity of fiber. Each core of MCF can accommodate single mode or number of modes depending on method of employing spatial multiplexing.

MCF was first discovered by Furakawa Electric in 1979. In 1990's investigations were carried out by France Telecom. However, further developments were not done. Research activity in MCF based systems started in late 2000's, due to saturation of SSMF based technologies at 100 Tb/s bit rates [12]. A typical seven-core MCF has one center core and six outer cores. Fig. 1.7 shows a schematic diagram of a 7 core MCF [13].

As shown in Fig.1.7, d is the centre core diameter. The diameters of all outer cores are deviated from center core diameter by amount δd . Λ is the distance between the two neighboring cores; it is also called core pitch. Core pitch defines the crosstalk between the neighboring cores. By altering the core pitch, crosstalk between neighboring cores can be changed. In the present case each core is surrounded by a trench [13]. Number of cores inside cladding of MCF depends on size of MCF and some other design parameters.

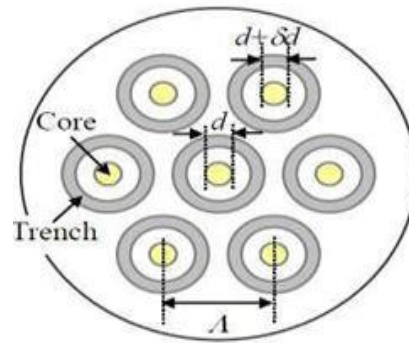


Fig. 1.7 Schematic of a 7-core MCF [13]

MCF is further of two types: solid and holey MCFs. Holey MCF is made from a **Photonic Crystal Fibre (PCF)**. PCF is a fibre that has hexagonal array of holes that run through entire length of the fiber. If a hole is omitted from its place, then it forms a core in PCF [14-15]. The MCF fabricated by omitting holes in PCF to form cores is shown below in Fig. 1.8 [14].

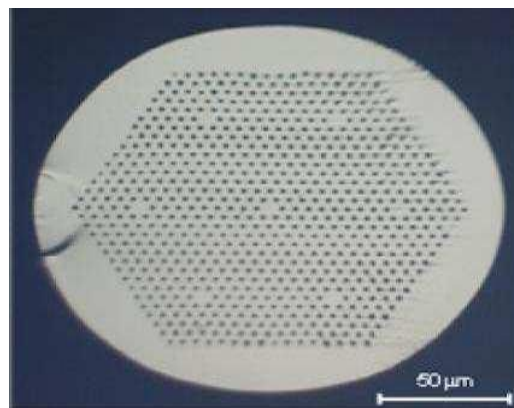


Fig. 1.8 Schematic of a holey MCF [14]

As shown in Fig. 1.8, in holey MCF, it's easy to incorporate cores wherever required in holey fibers as only requirement is omission of holes at respective position [15].

Further MCFs can be categorized into *homogeneous* and *heterogeneous* MCFs. In homogeneous MCF, all cores are identical to each other and core-to-core distance dominates the core density of MCF, which in turn ensures acceptable crosstalk level along a propagation length. In the case of heterogeneous MCF, all the cores are not identical to each other, as it is well known fact that maximum power transferred between cores goes down prominently if a cores have difference in their core

radius. So, in case of heterogeneous MCF, non-identical cores are arranged such that crosstalk between any pair of cores is small and cores are more efficiently packed as compared to homogeneous MCFs [1], [16].

In Fig. 1.9, different types of heterogeneous fibers are shown. Fig 1.9 (a) shows a 7-core heterogeneous MCF, in which three types of single mode cores are arranged in a triangular-lattice arrangement. The core pitch (Λ) is $40\ \mu\text{m}$ and core to core distance between identical cores is $69.3\ \mu\text{m}$. Fig. 1.9 (b) shows another arrangement of heterogeneous MCF called rectangular lattice arrangement. The core pitch (Λ) is $35\ \mu\text{m}$ and core to core distance is $70\ \mu\text{m}$, Fig 1.9 (c) and Fig 1.9 (d) shows the 19-core triangular arrangement and 12-core rectangular arrangement respectively [1].

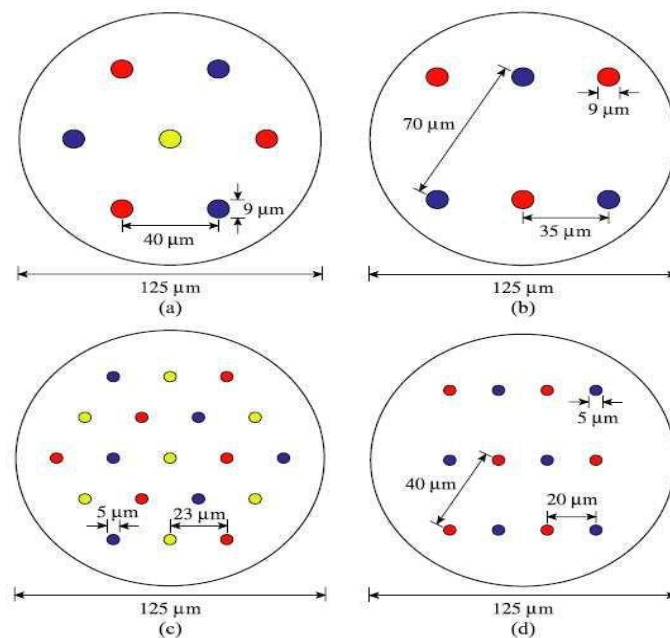


Fig. 1.9 Different types of Heterogeneous Fiber [13]

Single Mode MCF's (*SM-MCFs*) are characterized in terms of effective core area (A_{eff}), crosstalk and the number of cores. It can be classified according to parameters such as A_{eff} , crosstalk, cladding diameter, and the number of cores and core arrangement. Almost all the MCFs used the hexagonal close-packed structure (HCPS) [17]. The two-pitch structure (TPS) has large core pitch between a center core and outer cores [17]. The one-ring structure (ORS) is has no center core. Fig. 1.10 shows the cross sectional view of various MCF structure.

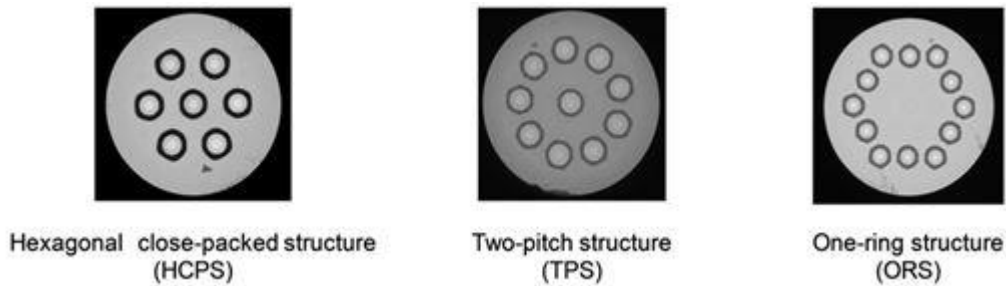


Fig. 1.10 Cross-sectional view of various structures of MCF's [17]

In Multimode Multicore fiber, (*MM MCF*) multi-core fiber and a multi-mode fiber is combined to expand the capacity of optical communication system [17]. Recently, the characteristics of fabricated Few Mode MCF (*FM-MCFs*) have been presented [17]. The key characteristic of designing a FM-MCF is the crosstalk related to higher modes. Few-mode fibers (FMFs) are demonstrated as a good compromise since they are sufficiently resistant to mode coupling compared to standard multimode fibers but they still can have large core diameters compared to single-mode fibers. As a result these fibers can have significantly less nonlinearity and at the same time they can have the same performance as single-mode fibers in terms of dispersion and loss. Fig. 1.11 shows the various types of MCF's.



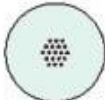
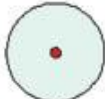
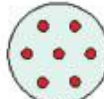
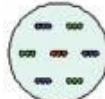
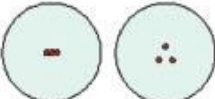
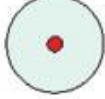

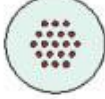
Number of modes	Single-core	Multi-core		
		Uncoupled-type	Coupled-type	
Single	SMF 	Homogeneous/Heterogeneous 		LMA fiber 
Few	FMF 	Few-mode MCF 	Hybrid structure 	Strongly/Weakly coupling 
Multi	MMF 	Multi-mode MCF 		LMA fiber 

Fig. 1.11 Various structures of MCF [13]

1.6.3.1 Applications of MCF

In the telecommunication sector, multicore fibers can be used to dramatically reduce the amount of space required and increase the bandwidth of the fiber-optic cable used in data center networks and exchanges. Data cables could be reduced in size by having, for instance, nineteen cores within one fiber. This would change the existing technology from a nineteen fiber ribbon to a single fiber cable, reducing the cross-sectional area and weight of the cable. Alternatively, the eight fibers could be replaced by nineteen multicore fibers, increasing the cable bandwidth nineteen times.

For applications in the biomedical sector, fiber Bragg gratings may be inscribed into each photosensitive core, providing the ability to use the fiber as a 3D shape sensor. Multicore fibers provide a platform for the next generation telecommunication devices and sensor systems. By combining multiple signal lines into a single connector space, space division multiplexing schemes can be utilized to save space and give high bandwidth cables. For the biomedical sector, the fiber has photosensitive cores, allowing Fiber Bragg Grating (FBG) inscription into each core, giving the ability to use the fiber as a 3D shape sensor, as deployed in catheters and other medical tools for minimally invasive procedures. It is also used in temperature and strain sensors. MCF is a promising candidate to enhance Optical Signal to Noise Ratio (OSNR) and avoid fiber fuse.

1.6.3.2. Limitations of MCF

- Densely arranged cores: design considerations are difficult.
- Inter-core crosstalk: Crosstalk severely affects the OSNR
- Leakage of light: causes noise for the center core.
- Increased mode coupling co-efficient: affects the signal quality.
- Detection of multi-signal requires sophisticated technology.
- Amplifiers and terminal equipment are complex.
- Modal dispersion caused by propagation in multiple modes having different group delays.

1.7 Multiplexing Techniques in Optical Communication System

Multiplexing is an essential part in a communication system where multiple users transmit data simultaneously through a single link, whether the link is a coaxial cable, a fiber, radio or satellite. Multiplexing is widely employed in communication systems due to its capability to increase the channel utilization or the transmission capacity and decrease system costs. There are various types of multiplexing techniques commonly used in optical fiber communication system, which working principles are discussed in the following subsections.

1.7.1 Wavelength Division Multiplexing (WDM)

In wavelength-division multiplexing (WDM) systems, different independent users transmit data over a single fiber using different wavelengths [7-8]. Conceptually, WDM scheme, which is illustrated in Fig. 1.12 is similar to frequency division multiplexing (FDM) used in microwave radio and satellite systems. At the transmitter side, n independent users' data are modulated onto n high frequency carriers, each with a unique wavelength (λ).

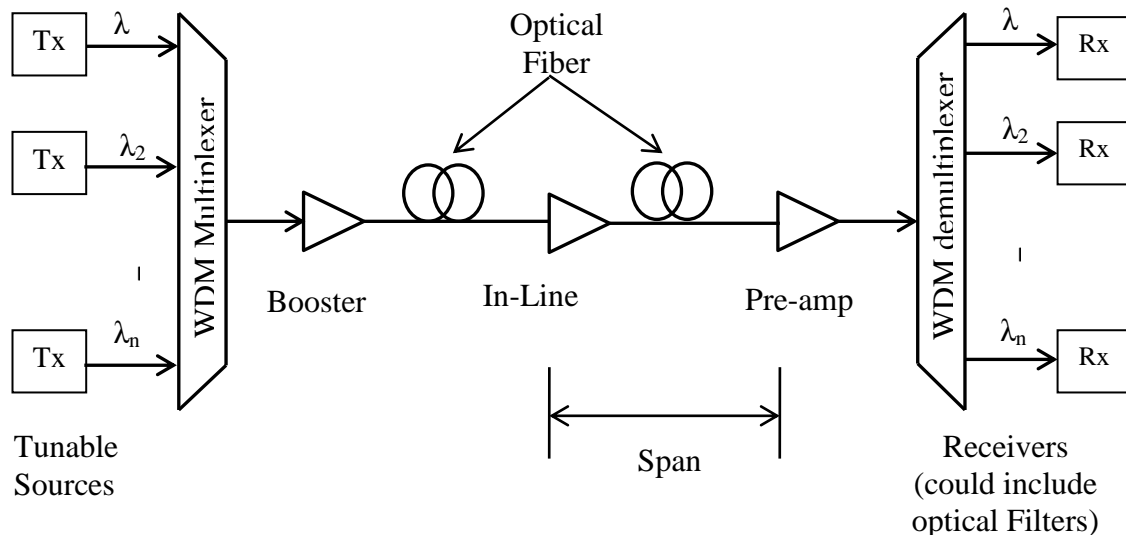


Fig. 1.12 Typical WDM Network [18]

These wavelengths can be spaced based on ITU-T standards. A wavelength multiplexer combines these optical signals and couples them into a single fiber. At the receiving end, a de-multiplexer is required to separate the optical signals into appropriate channels. This is done with n optical filters, whereby their cut-off frequency is set based on the transmitted light source frequency. The total capacity of a WDM link depends on

how close the channels can be spaced in the available transmission window. In late 1980s, with the advent of tunable LASER (Light Amplification by Stimulated Emission of Radiation) that have extremely narrow linewidth, one then can have very closely spaced signal bands. This is the basis of dense WDM (DWDM) [7]. Fig. 1.13 shows a typical WDM network containing various types of optical filter such as post-amplifier or booster, in-line amplifier and preamplifier.

1.7.2 Optical Frequency Division Multiplexing (Optical FDM)

Orthogonal Frequency Division Multiplexing (OFDM) plays a significant role in the modern telecommunications for both wireless and wired communications. Although OFDM has been studied in Radio Frequency (RF) domain for over four decades, the research on OFDM in optical communication began only in the late 1990s. OFDM was proposed as a way to overlap multiple channel spectra within limited bandwidth without interference, taking consideration of the effects of both filter and channel characteristics. It has few merits; Firstly, the frequency spectra of OFDM subcarriers are partially overlapped, resulting in high spectral efficiency. Secondly, the channel dispersion of the transmission system is easily estimated and removed, and thirdly, the signal processing in the OFDM transceiver can take advantage of the efficient algorithm of FFT/IFFT with low computation complexity. The basic concept of OFDM is quite simple: data is transmitted in parallel on a number of different frequencies, and as a result the symbol period is much longer than for a serial system with the same total data rate. Fig 1.13 describes the modulation and demodulation techniques of OFDM transmission.

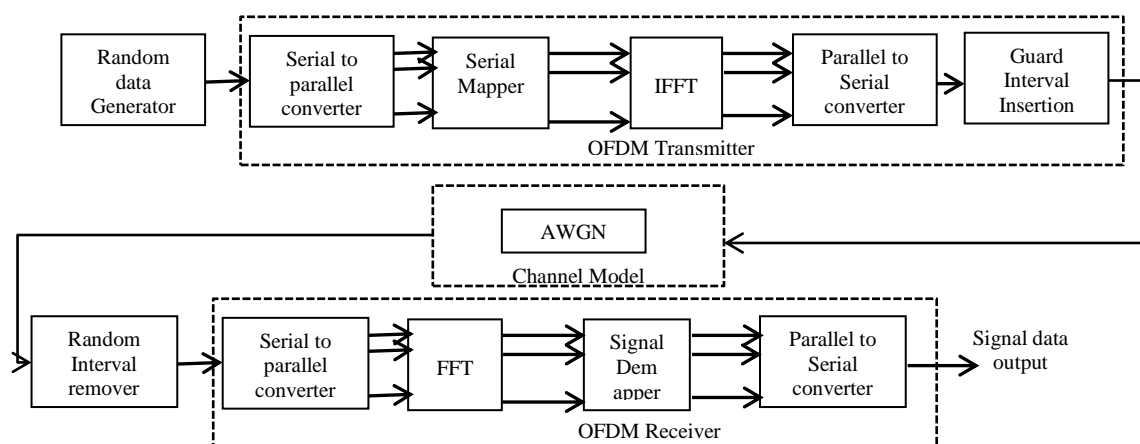


Fig. 1.13 Block Diagram of OFDM Modulation and Demodulation [18]

Optical FDM is two types: direct-detection optical OFDM (DDO-OFDM) looking into a simple realization based on low-cost optical components and coherent optical CO-OFDM aiming to achieve high spectral efficiency and receiver sensitivity [18].

Orthogonal frequency division multiplexing (OFDM) is a special form of a multi-carrier modulation (MCM) or subcarrier multiplexing (SCM). Basically OFDM is just plain old frequency-division multiplexing (FDM) with the orthogonality condition (7), namely $\Delta f = 1/T$. Where Δf is the subcarrier separation and T is the symbol duration. Since the symbol rate $R = 1/T$, we can also write $\Delta f = R$. In (O) FDM, multiple signals are transmitted using different carrier frequencies. Mathematically, with N sub-channels as

$$C(t) = \sum_{k=0}^{N-1} C_k(t) = \sum_{k=0}^{N-1} C_k(t) \cdot e^{(i\omega_k t)} \quad (1.1)$$

where the $f_k = \omega_k/2\pi$ fulfill the orthogonality condition above. Again, the c_k are the actual encoded data and the $C_k(t)$ are the subchannel symbols. The $C_k(t)$ can either be numbers in a processor that we use to generate our (O)FDM signal or electrical / optical field quantities which can simply be superposed as shown in above equation combining the fields from multiple sources.

In FDM/WDM there are frequency guard bands between the subcarriers. At the receiver the individual subcarriers are recovered using analog filtering techniques. In OFDM the spectra of individual subcarriers overlap, but because of the orthogonality property, as long as the channel is linear, the subcarriers can be demodulated without interference and without the need for analog filtering to separate the received subcarriers. OFDM principle is explained in Fig. 1.14.

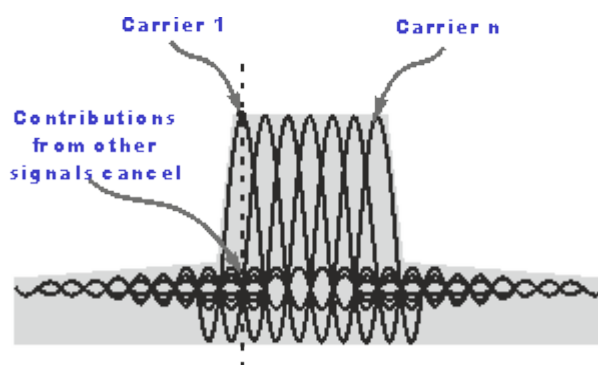


Fig. 1.14 OFDM Principle [7]

1.7.3 Mode Division Multiplexing (MDM)

A Mode is the path for light rays through an optical fiber. It is a solution of a wave equation describing a field distribution that propagates in a fiber without changing, except for an overall scaling that describes amplitude and phase changes. In an ideal fiber, modes propagate without cross-coupling. In a real fiber, perturbations, whether intended or unintended, can induce coupling between spatial and/or polarization modes. In a MMF with mode coupling, a pulse launched into an ideal mode couples into other modes, and a superposition of pulses with various group delay (GDs) is received. Mode coupling affects the transmission properties of fiber which is a serious cause for concern when used for long distance communication. Mode coupling leads to intramodal dispersion like material dispersion and waveguide dispersion and also intermodal dispersion.

Orthogonality between modes in a highly multimodal waveguide can be exploited to submit independent data streams over different mode groups which are referred as *mode group multiplexing or the mode division multiplexing (MDM)*. In the mode-division multiplexing optical transmission system, a mode multi/demultiplexer is an important key device for excitation, multiplication, and separation of light signals which have distinct modes. In MMF, a plurality of modes typically leads to *modal dispersion*, limiting the bit rate \times distance product of direct-detection systems, so it was long viewed as a strictly negative effect. This plurality is now seen as increasing capacity through *mode-division multiplexing (MDM)* [19].

1.7.3.1 Application of MDM

In mode-division-multiplexed systems using coherent detection, strong mode coupling is beneficial. Mode coupling reduces modal dispersion, minimizing signal processing complexity. In combination with modal dispersion, mode coupling creates frequency diversity, mitigating the mode-dependent gain of optical amplifiers.

Spatial Division Multiplexing (SDM) with Multi-Core Fibers (MCFs) is a promising candidate technology with which to overcome the capacity limit of current optical communication systems.

In MDM using coherent detection, one can employ a fixed set of D orthogonal modes (e.g., ideal modes) as transmit and receive bases, and perform frequency-dependent $D \times$

D matrix signal processing to approximately invert the propagation operator. Recently a group of researcher's from Netherlands demonstrated the viability of spatial multiplexing to reach a data rate of $5.1 \text{ Tbit s}^{-1} \text{ carrier}^{-1}$ (net $4 \text{ Tbit s}^{-1} \text{ carrier}^{-1}$) on a single wavelength over a single fibre [20]. Furthermore, by combining this approach with wavelength division multiplexing with 50 wavelength carriers on a dense 50 GHz grid, a gross transmission throughput of 255 Tbit s^{-1} (net 200 Tbit s^{-1}) over a 1 km fibre link is achieved.[20-21].

1.7.4 Optical Code Division Multiple Access (Optical CDMA)

Optical CDMA is a code division multiplexing technology that allows several transmitters to transmit simultaneously on an **optical** fiber. Nodes transmit using code words from an Optical Orthogonal Codeset (OOC) [22]. An OOC is a set of (0, 1) sequences of length N that satisfies certain autocorrelation and cross-correlation constraints. The term codeset is used to refer to the set of such sequences, and the term code word is used for a member of the set. Each 0 or 1 of a sequence is called a chip, and the sequence represents a data bit. The number w of 1 chips of a code word of the codeset is called its Hamming weight. A node transmits data by ON-OFF keying (OOK) of a code word. Optical CDMA receivers are correlation receivers. By connecting nodes on the network in a star, bus or ring topology any node can transmit to any other using the receiver's code word. The advantage of optical CDMA is that it allows utilization of the available transmission capacity of an optical fiber. Data processing can occur at electronic speeds while encoding and decoding can be done all optically at a higher chipping rate. The users are assigned unique codes which act as addresses. The codes are unique in the sense that the matched receiver with a matched code word will receive the transmissions correctly whereas the receiver with unmatched code will not be able to listen to the transmission. Hence optical CDMA becomes a suitable multiple access technology where only the desired receiver will be able to listen to the transmission [22]. The codes used as addresses are obtained from some code family designed to satisfy some basic properties which are Off-peak autocorrelation, cross-correlation, code weight and code length so as to yield the desired system performance at the given data rates. The main problem with using optical CDMA in a LAN is that at high loads, multiuser interference errors result in low network throughput.

1.8 Previous Works

The study of BER in optical fiber communication links is of great interest for the design of MCF optic communication systems. One of the major system-level requirements that motivate the design of optical links is the BER. MCF's is used in large capacity transmission system and the signal integrity in MCF is affected by crosstalk between different cores, which arises due to power coupling between the cores during the signal propagation. The crosstalk grows with the mode overlap and decreases with the core separation.

M. Koshiba et al. [1] suggested a new type of optical fiber called heterogeneous multi-core fiber (heterogeneous MCF) for large-capacity optical-transport networks. In the heterogeneous MCF, not only identical but also non-identical cores, which are single-mode in isolation of each other, are arranged so that cross-talk between any pair of cores becomes sufficiently small.

Y. Kokubun et al. [2] has proposed another new type of MCF called homogeneous multi-core fiber (MCF) to drastically increase the transmission capacity of single fiber using the MDM. This type of MCF utilizes the coupling between adjacent cores in a positive manner. In the homogeneous MCF, cores with identical index contrast and index profile are closely arranged so that the cores are strongly coupled to each other to form coupled modes, each of which corresponds to a transmission channel.

T. Morioka et al. [3] summarizes all the recent articles in optical fiber communication system that reviews the most recent research efforts around the globe launched over the past few years with a view to overcome the limitations faced so far and substantially increase capacity by exploring the last degree of freedom available: the spatial domain. Central to this effort has been the development of brand new fibers for space-division multiplexing and mode-division multiplexing.

S.Ö.Arık et al. [11] discussed about Coupled-core MCFs that offer characteristics which are beneficial for long-haul spatially multiplexed transmission. Coupled-core (CC) MCFs present an alternative for spatial multiplexing which can be considered as a form of Multi-mode fibers (MMFs). MMF uses the plurality of modes as parallel channels.

K.Imamura, R.Sugizaki [12] summarized the progresses of multi-core fibers for ultra-high capacity transmission systems. Recent efforts, reliability issues and splicing technique for multi-core fibers are also described in this paper.

K.Takenaga et al. [13] proposed a trench-assisted multi-core fiber (TA-MCF) to achieve high dense MCF design with a solid structure. The crosstalk value at 1.55 μm of fabricated TA-MCF is estimated to be -35 dB at 100 km. The proposed method is a good option to reduce crosstalk in MCF.

K.Mukasa et al. [14] introduced the developments of multi-core fibers, both solid type and holey type. The SDM is realized by the MCF to enhance the transmission capacity.

D.M. Taylor et al. [15] demonstrated a novel micro-structured fibre for use in an optical interconnection system. The demonstration of feasible multichannel communication with acceptably low crosstalk has been successfully achieved with a specifically designed multi-core photonic crystal fibre (PCF) and butt-coupling to vertical-cavity surface-emitting laser (VCSEL) arrays.

M. Koshiha [16] reviewed the recent progress in MCF for ultra large capacity transmission. In addition to a traditional, homogeneous MCF with identical cores, a new type of MCF called heterogeneous MCF with not only identical, but also non-identical cores is introduced.

S. Matsuo et al. [17] reviewed the research activities concerning multi-core fiber, few-mode fiber and few-mode multi-core fiber. The characteristic of the 12-core fiber that was used for the first 1-Pb/s/fiber transmission experiments is presented.

J. M. Khan et al. [19] analyzed the mode coupling effects in a mode-division-multiplexed systems using coherent detection. They found strong mode coupling as beneficial. They also explained that mode coupling reduces modal dispersion, minimizing signal processing complexity. In combination with modal dispersion, mode coupling creates frequency diversity, mitigating the mode-dependent gain of optical amplifiers.

R. G. H. van Uden et al. [20] demonstrated few-mode multicore fibre, by employing compact three-dimensional waveguide multiplexers and energy-efficient frequency-

domain multiple-input multiple-output equalization, the viability of spatial multiplexing to reach a data rate of $5.1 \text{ Tbit s}^{-1} \text{ carrier}^{-1}$ (net $4 \text{ Tbit s}^{-1} \text{ carrier}^{-1}$) on a single wavelength over a single fibre. Furthermore, by combining this approach with wavelength division multiplexing with 50 wavelength carriers on a dense 50 GHz grid, a gross transmission throughput of 255 Tbit s^{-1} (net 200 Tbit s^{-1}) over a 1 km fibre link is achieved.

M. Sakauchi et al. [21] have succeeded to develop a prototype 19-core EDFA (erbium-doped fiber amplifier) for demonstrating the principle of simultaneous pumping which enables long-distance optical transmission with a large capacity equivalent to 19 individual optical fibers. The 19-core simultaneous pumped optical amplifier is capable of simultaneously amplifying optical signals transmitted through 19 cores. The technology is a leap forward in the practical realization of large-capacity, long-distance optical communication using multicore fibers.

J. Singh [22] narrated different fundamental techniques of encoding/decoding in optical CDMA systems.

Y. Kokubun et al. [23] successfully demonstrated the selective excitation of coupled modes in a homogeneous coupled multi-core fiber for the first time. Coupled modes of homogeneous coupled MCF are selectively excited and discriminated utilizing the difference of equivalent propagation angle.

A. W. Snyder [24] derived a set of coupled-mode equations to describe mode propagation in uniform and slightly non-uniform cylindrical optical-fiber systems. The coupling between fibers of an array made up of n identical fibers each at the vertex of a polygon and one at the center, which is not necessarily the same as its n neighbors, is determined. Mode coupling on a lossy fiber is investigated and a simple expression for the loss of a HE_{11} mode is given.

H. A. Haus et al. [25] investigated coupled-mode equations for systems of four and five planar coupled waveguides to determine transmission characteristics of interest. By proper selection of the coupling coefficients in a system of "synchronous" waveguides, full transfer can be achieved from one outermost guide to the guide on the opposite side. In the five-waveguide system, an excitation of the center guide can be fully transferred to a symmetric excitation of the outer guides.

F. Y. M. Chan et al. [26] analytically derived the propagation dynamics of 7-core multi-core fibers (MCFs) with identical and three-types of cores basing on the coupled-mode theory. With mode coupling as cross-talks in a communication theory framework, joint signal processing techniques for crosstalk mitigation and characterize corresponding transmission performance was studied. For MCFs with homogeneous cores, they showed that the coupling dynamics are aperiodic in general. For MCFs with heterogeneous cores, it is found that even though signals from different core groups will not couple with each other, the coupling within their own group is significantly affected by the presence of other core groups. The analytical insights obtained provide a more complete understanding of signal transmission and cross-talks in MCFs. It is shown that aperiodic mode coupling in intensity modulated systems induces crosstalk's that are difficult to eliminate through signal processing. For intensity modulated systems, the aperiodic coupling dynamics prevent complete mitigation of cross-talks and lower bounds on the system BER are determined.

F. Yaman et al. [28] proposed multimode fibers for long-haul transmission and demonstrated experimentally. They have shown that few-mode fibers can be used for long-distance transmission without modal dispersion or insertion loss penalty. In particular the experimental results show that no mode coupling is observed in 35-km-long few-mode fiber and after 1050 km of transmission in a recirculating loop. Few-mode fibers (FMFs) are demonstrated as a good compromise since they are sufficiently resistant to mode coupling compared to standard multimode fibers but they still can have large core diameters compared to single-mode fibers. As a result these fibers can have significantly less nonlinearity and at the same time they can have the same performance as single-mode fibers in terms of dispersion and loss.

T. Hayashi et al. [29] designed and fabricated a low-crosstalk seven-core fiber with transmission losses of 0.17dB/km or lower. They also investigated the signal-to-noise ratio (SNR) achievable in uncoupled multicore transmission systems by regarding the crosstalk as a virtual Additive White Gaussian Noise (AWGN). They explained that SNR enhancement in each core of the MCF can be realized by improving transmission loss and by finding a good balance between large effective area and low crosstalk, so that the SNR under crosstalk can be maximized.

S. M. Jahangir Alam et al. [30] suggested different modulation techniques scheme for improvement of BER in fiber optic communications. The developed scheme has been tested on optical fiber systems operating with a non-return-to-zero (NRZ) format at transmission rates of up to 10 Gbps. Performance of improved detected signals has been evaluated by the analysis of quality factor and computed BER. The optimum solution reduces the BER by using RZ signal generator through Electro-Absorption modulation techniques.

We have observed from the above mentioned works that different researchers investigated and followed different methods, techniques and tools to analyze system performance of an optical fiber transmission system. Some of the research works were carried out analytically, numerically or experimentally. From the above literature review, we have observed that most of the research works have analyzed the MCF as a high speed medium and discussed the effect of crosstalk and noise due to adjacent cores. In this thesis work also, we have studied the MCF as a transmission media by changing different parameters values such as distance, coupling coefficient, input power, gain etc to evaluate system performance.

1.9 Objectives of the Thesis

The objectives of the research work are:

- (i) To carryout analytical development to determine the expressions of optical signal power and crosstalk power at the output of a single mode multicore fiber with specific fiber structure and fiber length and to evaluate the optical signal to crosstalk ratio (SCR) at the output of an optical MCF link for a given fiber structure.
- (ii) To derive the expressions for photocurrent due to signal, crosstalk and beat noise current at the output of an optical receiver with a PIN photodiode;
- (iii) To evaluate electrical SCNR and the bit error rate (BER) analytically in presence of crosstalk and to determine the optimum system parameters for a given system BER of 10^{-9} and a given data rate. Further to determine the penalty due to crosstalk and maximum allowable transmission distance for a given input optical power and BER.

The outcome of this research work will be useful to design fiber optic system with Multi-core Multi-mode fiber running at BER comparable to single mode fiber links.

1.10 Organization of the Thesis

This thesis is divided in four chapters. At the beginning of **Chapter 1** General description of optical fiber communication system is presented. Then types, generations of optical fiber communication system, along with their application and limitations are described. Optical fiber properties (refractive index of fibers, fiber modes etc) and description of MCF, PCF, and optical Multiplexing Techniques (MDM, OFDM, Optical CDMA etc) are presented. Then an elaborate record of previous works on the analysis of multicore optical fiber communication system is presented. Objectives of the thesis are formulated here.

Chapter 2 Provides the configuration of system model. Analysis of the model and its important parts; transmitter and receiver block diagram is described. Derivation of signal power and crosstalk power, noises in the receiver and amplifier, Signal to Crosstalk Ratio (SCR), Signal to Crosstalk plus Noise Ratio (SCNR) are carried out. Computations of BER for various system parameters such as input power, coupling coefficient, transmission distance, data rate, and optical pre-amplifier gain are done here.

Chapter 3 Presents the Results and Discussion. We plot some graph based on our theoretical analysis explained at chapter 2.

Chapter 4 Presents the conclusive remarks of this thesis along with the scope of future research work.

CHAPTER 2

ANALYSIS OF OPTICAL LINK WITH MCF

2.1 Introduction

In this chapter a system model is considered for an optical link using a multi core single mode (MC-SMF) fibre. The system analysis is then carried out to find the signal power and crosstalk power at the output of MCF. BER expression is also developed for an intensity Modulated (IM) On-Off Keying (OOK) signal.

2.2 System Model

Fig. 2.1(a) and Fig. 2.1(b) shows an MCF composed of seven identical cores (labeled core 1, 2, ..., 7) arbitrarily embedded near the center of the cladding. The p^{th} core is identified by its radius and refractive index as a_p and n_{1p} respectively while the cladding has a refractive index of n_2 . The cores are spatially positioned such that the field from each core is relatively well isolated and perturbation methods with conventional coupled-mode theory can be used to analyze the mode coupling dynamics. From the system model, power at the centre core and also total interference crosstalk coupled to the centre core due to other outer cores can be calculated.

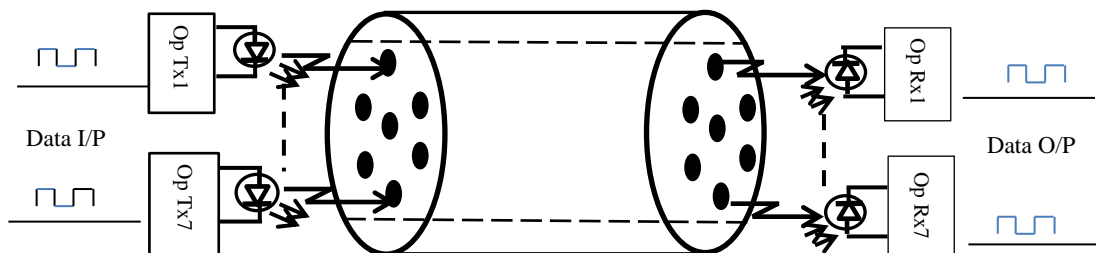


Fig. 2.1(a) Block diagram of an Optical MIMO Link with MCF without Pre-Amplifier

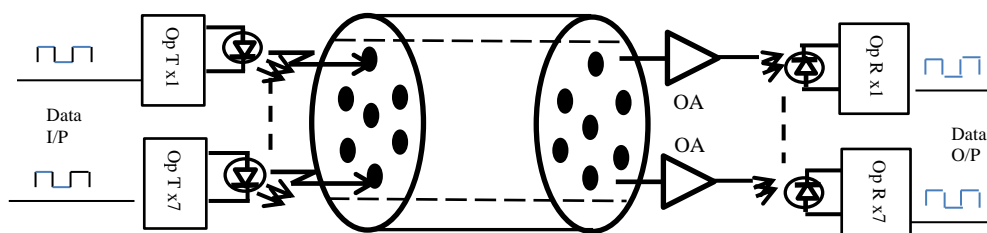


Fig. 2.1(b) Block diagram of an Optical MIMO Link with MCF with Pre-Amplifier

Each core of the seven cores MCF has a radius of ‘ a ’ and separated by $\Lambda = 30\text{-}\mu\text{m}$ core-to core pitch. The MCF is designed for single-mode operation in the 1550 nm transmission window and is made of seven 8- μm core diameter cores arranged in a triangular array. The glass cladding diameter is 125 μm and the acrylate dual coating diameter is 250 μm . The cutoff wavelength for each core is about 1200 nm and mode field diameters (MFD) is 10.2 μm approximately. All cores have refractive index 1.51 and cladding have the refractive index of 1.44. Seven optical transmitters are connected to seven data channel of the system. For the purpose of the analysis, simultaneous launching of light to all the cores are not considered, only the centre core is given with the OOK data for calculating the power coupled to the centre core and for calculating the inference crosstalk to the centre core it is considered that outer cores are given power input. The cores are terminated by seven detectors and seven optical receivers to receive the data bits. Data output is taken from the center core or the core under test at a particular time. Signal power for the centre core is derived and then interference crosstalk power to the centre core due to other cores is evaluated. Signal to Crosstalk Ratio (SCR) is then computed from signal power and crosstalk power. Finally, BER is derived from the SCR for other fiber parameters.

2.2.1 Transmitter Block Diagram

The main parts of the transmitter section are a source (either a **LED** or a **LASER**); efficient coupling means to couple the output power to the fiber, a modulation circuit and a level controller for LASERs. In present days, for longer repeater spacing, the use of single mode fibers and LASERs seem to be essential whereas the earlier transmitters operated within 0.8 μm to 0.9 μm wavelength range, used double hetero structure LASER or LED as optical sources. High coupling losses result from direct coupling of the source to optical fibers. Fig. 2.2 shows the various parts of a fibre optic transmitter.

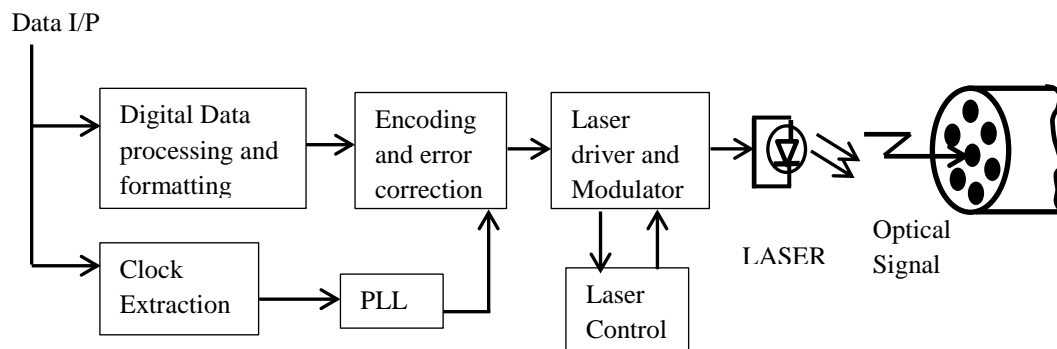


Fig. 2.2 Transmitter Block Diagram [5]

The **transmitter** has got two parts, the first part receives the signal, process it and modulate as necessary; the second part directs the optical transmitter to turn the light "on" and "off" in the correct sequence, thereby generating a light signal. The transmitter is physically close to the optical fiber and may even have a lens to focus the light into the fiber. LASERs have more power than LEDs, but vary more with changes in temperature and are more expensive. The most common wavelengths of light signals are 850 nm, 1,300 nm, and 1,550 nm (infrared, non-visible portions of the spectrum).

Basic functions of transmitters are:

- Digital Data processing and formatting
- Encoding of input data
- Error correction
- Line coding to control transmitted spectrum
- Electronic to optical conversion

In a transmitter most important task is the modulation. Most common form of modulation is intensity modulation (IM) and on-off keying (OOK) which can be carried out electrically or optically. The transmitted signal is a two-level binary Non Return to Zero (NRZ) data stream of duration T_b . This time slot is referred as *bit period*. There are many ways of sending a given digital message; one of the simplest techniques for sending binary data is *amplitude shift keying* (ASK) or *on-off keying* (OOK), wherein a voltage level is switched between two values, which are usually on or off. The resultant signal wave thus consists of a voltage pulse of amplitude V relative to the zero voltage level when a binary 1 occurs and a zero-voltage-level space when a binary 0 occurs. Depending on the coding schemes to be used, a binary 1 may or may not fill the same slot T_b . For simplicity, we can assume that when 1 is sent, a voltage pulse of duration T_b occurs, whereas for 0 the voltage remains at its zero level.

$$m(t) = \begin{cases} 1, & \text{symbol 1} \\ 0, & \text{symbol 0} \end{cases}$$

The function of the optical transmitter is to convert the electrical signal to an optical signal. By directly modulating the light source drive current with the information stream to produce a varying optical output power $P(t)$. Thus, in the optical signal emerging from the LED or laser transmitter, 1 is represented by a pulse of signal power (light) of duration T_b , where 0 is the absence of light. The optical signal that is coupled

from the light source to the fiber becomes attenuated and distorted as it propagates along the fiber waveguide. Upon arriving at the end of the fiber, a receiver converts the optical signal back to an electrical format.

2.2.2 Block Diagram of Optical Receiver with Optical Pre-Amplifier

The optical receiver takes the incoming digital light signals, decodes them and sends the electrical signal to the other user's computer, TV or telephone. The receiver uses a **photocell** or **photodiode** to detect the light. Functions of receiver are:

- A photodiode to provide optical to electronic conversion
- Linear circuitry to regenerate the data signal with minimal error
- Post regeneration processing (e.g. for error detection)

The optical signal at the receiving end is usually very weak after travelling along the fiber and an optical pre-amplifier may be used before the photodetector. Fig. 2.3 shows the basic components of an optical receiver. The first element is either a *pin* or an avalanche photodiode, which produces an electric current that is proportional to the received power level. Since this electric current typically is very weak, a *front-end* amplifier boosts it to a level that can be used by the subsequent electronics.

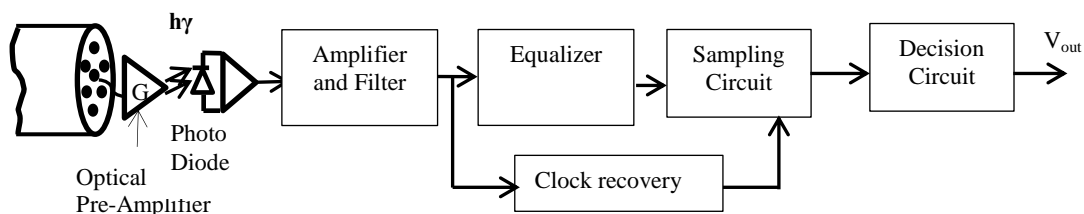


Fig 2.3 Receiver block Diagram [5]

After the electric signal produced by the photodiode is amplified, it passes through a *low-pass filter* to reduce the noise that is outside of the signal bandwidth. This filter thus defines the receiver bandwidth. In addition, to minimize the effects of inter symbol interference (ISI) the filter can reshape the pulses that have become distorted as they travel through the fiber. This function is called equalization since it equalizes or cancels pulse-spreading effects.

In the final stage of the optical receiver, a decision circuit samples the signal level at the midpoint of each time slot and compares it with a certain reference voltage known as

the threshold level. If the received signal level is greater than the threshold level, 1 is said to have been received. If the voltage level is below the threshold level, 0 is assumed to have been received. To accomplish this bit interpretation, the receiver must know where the bit boundaries are. This is done with the assistance of a periodic waveform called a clock, which has a periodicity equal to the bit interval. Thus, this function is called *clock recovery* or *timing recovery*.

In some cases, an optical preamplifier is placed ahead of the photodiode to boost the optical signal level before photo detection takes place. This is done so that Signal to Noise Ratio degradation caused by the thermal noise in the electronics can be suppressed. Compared with other front-end devices, such as avalanche photodiodes or optical heterodyne detectors, an optical preamplifier provides a larger gain factor and a broader bandwidth. However, this process also introduces additional noise to the optical signal.

Detection in the system can be incoherent, referred to as direct detection, or coherent which requires the presence of a laser diode local oscillator at the receiver, similar to radio communication. Direct detection is used in most practical systems since it is difficult to generate a stable carrier oscillator (laser) at the receiver which is matched with that at the transmitter. Fiber systems employ direct detection with amplitude shift keying (ASK) commonly called on-off-keying (OOK) or Intensity Modulation (IM) since the laser is turned ‘on’ to transmit a ‘1’ and turned ‘off’ to indicate a ‘0.’

2.3 System Analysis

2.3.1 Mode Coupling Theory in a Seven Core MCF

In this system we analytically study the propagation dynamics of the 7-core MCFs which has a center core (namely, core 1) surrounded by six cores (namely, core 2, 3, ..., 7) arranged in a triangular lattice as shown in Fig. 2.4. We assume that each core only supports the LP_{01} fundamental mode and we denote the amplitude of the p th core as $A_p(z)$. Electrical data input when passed to optical transmitter, it converts the electrical signal to optical signal. The optical signal is launched to the centre core of the designed 7 x 7 MCF through the LED or a LASER source. Optical power when propagate through the fiber core, it induces power to other cores of the MCF [23]. The mode power of a particular core is affected by the power induced from other core and as a result **mode coupling** phenomenon takes place. The simultaneous mode coupling between all the

cores of a MCF is governed by a set of coupled- mode equations [24-25], which can be written in a matrix form as

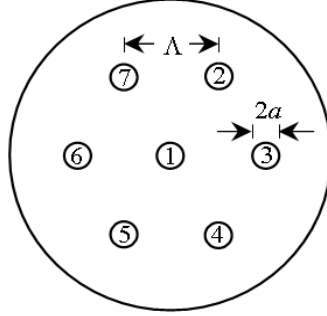


Fig. 2.4 Homogeneous 7-core MCF with core radius ‘a’

$$\frac{d\mathbf{A}(z)}{dz} = -\mathbf{C}\mathbf{A}(z) \quad (2.1)$$

where $\mathbf{A}(z) = [A_1(z) A_2(z) \dots A_n(z)]^T$ is a column vector and T denotes the transpose, z is the direction of propagation, and \mathbf{C} is a $n \times n$ matrix with elements C_{pq} given by [26]

$$C_{pq} = \begin{cases} jC_{pq} \exp[j(\beta_p - \beta_q)z] & p \neq q \\ 0 & p = q \end{cases} \quad (2.2)$$

where β_p represents the propagation constant for the LP_{01} mode of core p . The coupling coefficient (C_k) between p^{th} and q^{th} core, C_{pq} is a measure of the spatial overlapping of the mode fields of core p and q over the cross-sectional area of core q . Using the addition theorem to express the mode field of core p in terms of the local coordinate system of core q and with the help of the eigenvalue equation for a step-index optical fiber C_{pq} can be obtained from equation (2.3) [27].

$$C_{pq} = \sqrt{2\Delta_q} W_q U_p K_0 \left(\frac{W_p d_{pq}}{a_p} \right) \left[a_p U_q J_1(U_q) I_0 \left(\frac{W_p a_q}{a_p} \right) + a_q W_p J_0(U_q) I_1 \left(\frac{W_p a_q}{a_p} \right) \right] \quad (2.3)$$

$$[V_p J_1(U_q) K_1(W_p) (a_q^2 U_q^2 + a_q^2 W_p^2)]^{-1}$$

where J_l , I_l and K_l are the Bessel function of the first kind and the modified Bessel functions of the first and second kinds of order l respectively and d_{pq} is the distance between the centres of the core p and core q . The normalized fiber parameters U_p , V_p and W_p are defined as $U_p = a_p [(2\pi n_{1p} / \lambda)^2 - \beta_p^2]^{1/2}$, $V_p = a_p (2\pi / \lambda) (n_{1p}^2 - n_2^2)^{1/2}$,

$W_p = a_p [\beta_p^2 - (2\pi n_2 / \lambda)^2]^{1/2}$ with λ being the free-space wavelength. The index constant can be measured by $\Delta_p = (n_{1p}^2 - n_2^2) / (2n_{1p}^2)$ and can be approximated as $(n_{1p} - n_2) / n_{1p}$, which corresponds to the relative core-cladding index difference. For simplicity and from [26] we shall only take a range of optimum values of C_{pq} from 0.5 to 2.5 for our analysis. The electric field of the individual core, denoted as $E_p(z)$, can be expressed in terms of its mode amplitude $A_p(z)$ as [26]

$$E_p(z) = A_p(z) \exp(-j\beta_p z) \quad (2.4)$$

Equation (2.1) cannot be solved readily because the elements in \mathbf{C} are z -dependent. Using equation (2.4), we can translate equation (2.1) to an eigenvalue problem

$$\frac{d\mathbf{E}(z)}{dz} = -\mathbf{R}\mathbf{E}(z) \quad (2.5)$$

where $\mathbf{E}(z) = [E_1(z) \ E_2(z) \ \dots \ E_n(z)]^T$ and \mathbf{R} contains z -independent elements r_{pq} given by

$$r_{pq} = \begin{cases} jC_{pq} & p \neq q \\ j\beta_p & p = q \end{cases} \quad (2.6)$$

Using the substitution $\mathbf{E}(z) = \exp(-\mathbf{R}z)\mathbf{E}(0)$, the solution to equation (2.5) is obtained as

$$\mathbf{E}(z) = \mathbf{V}[\exp(-\gamma_p)\delta_{pq}] \mathbf{V}^{-1}\mathbf{E}(0) \quad (2.7)$$

and

$$\mathbf{V} = [\mathbf{v}_1 \ \mathbf{v}_2 \ \dots \ \mathbf{v}_n] \quad (2.8)$$

Where δ_{pq} is the Kronecker delta function, γ_p is an eigenvalue of \mathbf{R} , and \mathbf{v}_p is the corresponding eigenvector. Equation (2.7) is a generalized solution for an n -core MCF that describes the power exchange between the modes of individual cores as the light propagates.

For the simplest configuration of the seven core MCF that is $\Delta_p = \Delta$ for all p , i.e. a homogeneous 7-core MCF as shown in Fig. 2.4, the coupled mode equations are given by equation (2.1) with the matrix

$$\mathbf{C} = j \begin{pmatrix} 0 & C_{12} & C_{12} & C_{12} & C_{12} & C_{12} & C_{12} \\ C_{12} & 0 & C_{12} & 0 & 0 & 0 & C_{12} \\ C_{12} & C_{12} & 0 & C_{12} & 0 & 0 & 0 \\ C_{12} & 0 & C_{12} & 0 & C_{12} & 0 & 0 \\ C_{12} & 0 & 0 & C_{12} & 0 & C_{12} & 0 \\ C_{12} & 0 & 0 & 0 & C_{12} & 0 & C_{12} \\ C_{12} & C_{12} & 0 & 0 & 0 & C_{12} & 0 \end{pmatrix}$$

where the off-diagonal zeros correspond to pairs of cores assumed to have negligible coupling due to large inter-core distances. Translating \mathbf{C} into \mathbf{R} using equation (2.6) yields a sequence of eigenvalues in increasing mode order given by

$$\gamma_1 = jC_{12}(1 + \sqrt{7}), \gamma_2 = \gamma_3 = jC_{12}, \gamma_4 = \gamma_5 = -jC_{12}, \gamma_6 = jC_{12}(1 - \sqrt{7}), \gamma_7 = -2jC_{12} \quad (2.9)$$

When light is launched into core 1 (centre core), i.e. $A_1(0) = 1$ and $A_p(0) = 0$ for $p \neq 1$, analytical solution for the mode amplitude at distance z are obtained as [26].

$$A_1(z) = [\cos(\sqrt{7} C_{12}z) + \frac{j}{\sqrt{7}}(\sin(\sqrt{7} C_{12}z))]e^{-jC_{12}z} \quad (2.10)$$

and

$$A_p(z) = -\frac{j}{\sqrt{7}}(\sin(\sqrt{7} C_{12}z))]e^{-jC_{12}z} \quad p \neq 1 \quad (2.11)$$

When light is launched into core 2, i.e. $A_2(0) = 1$ and $A_p(0) = 0$ for $p \neq 2$, the mode amplitudes for various core are given by [26].

$$A_1(z) = -\frac{j}{\sqrt{7}}(\sin(\sqrt{7} C_{12}z))]e^{-jC_{12}z} \quad (2.12)$$

$$A_2(z) = \frac{2}{3}\cos(C_{12}z) + \frac{1}{6}e^{2jC_{12}z} + \frac{1}{6}e^{-jC_{12}z}[\cos(\sqrt{7}C_{12}z) - \frac{j}{\sqrt{7}}(\sin(\sqrt{7}C_{12}z))] \quad (2.13)$$

$$A_3(z) = -\frac{j}{3}\sin(C_{12}z) + \frac{1}{6}e^{(2jC_{12}z)} + \frac{1}{6}e^{(-jC_{12}z)}[\cos(\sqrt{7}C_{12}z) - \frac{j}{\sqrt{7}}(\sin(\sqrt{7}C_{12}z))] \quad (2.14)$$

$$A_4(z) = -\frac{1}{3}\cos(C_{12}z) + \frac{1}{6}e^{(2jC_{12}z)} + \frac{1}{6}e^{(-jC_{12}z)}[\cos(\sqrt{7}C_{12}z) - \frac{j}{\sqrt{7}}(\sin(\sqrt{7}C_{12}z))] \quad (2.15)$$

$$A_5(z) = -\frac{j2}{3}\sin(C_{12}z) - \frac{1}{6}e^{(2jC_{12}z)} + \frac{1}{6}e^{(-jC_{12}z)}[\cos(\sqrt{7}C_{12}z) - \frac{j}{\sqrt{7}}(\sin(\sqrt{7}C_{12}z))] \quad (2.16)$$

$$A_6 = A_4$$

$$\text{and } A_3 = A_7;$$

The propagation dynamics of a 7 core MCF when light is launched into core 2 or any core other than the centre core are shown in Fig 2.5 [26].

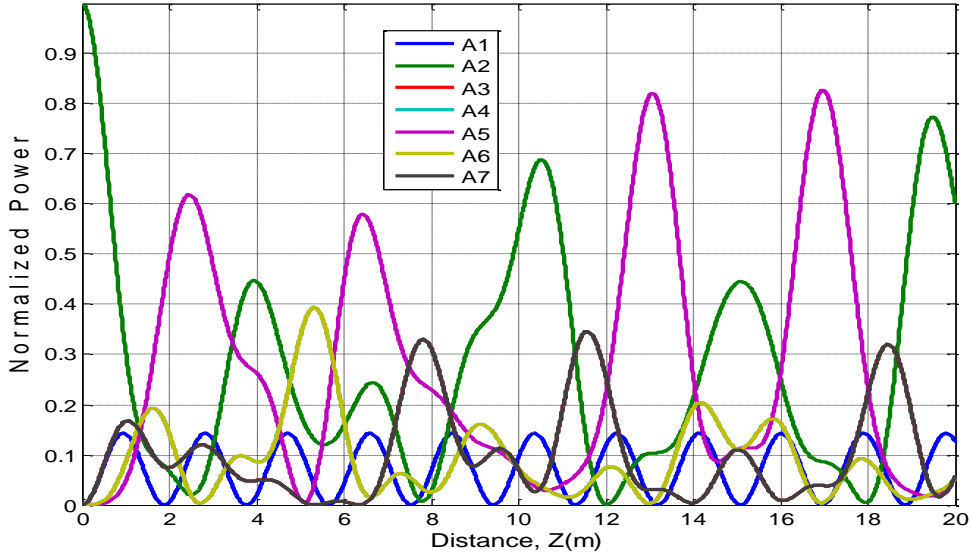


Fig. 2.5 Coupling dynamics of a 7 core MCF [26]

Some of the mode amplitudes are identical due to symmetry. In addition to unequal coupling to different cores, launching into core 2 (or other outer cores) also leads to aperiodic coupling for all the cores except the center core. From the communication theory perspective, aperiodic mode coupling results in cross-talks in the MIMO MCF system that is aperiodic over transmission distance. To describe aperiodic mode coupling dynamics a generalized coupling length L_{cp} is introduced in figure 2.5. L_{cp} is defined as the propagation length at which the normalized mode power in the p_{th} launching core drops from one to its first minimum. This definition is in general as it incorporates both aperiodic and periodic coupling dynamics. The coupling length for core 2 is calculated numerically from equation (2.13) by setting its first derivative $dA_2(z)/dz|_{z=L_{c2}} = 0$ which is given by

$$L_{c2} = 1.585/C_{12}. \quad (2.17)$$

Most of the recent reported analysis on mode coupling in MCF's as transmission fibers utilizes a 2 or a 3 core model [2] [14] [26,28-29] and gives a description on mode coupling effects, but mode power and interference crosstalk power calculation due to six outer cores is not done. The BER analyses of a seven core MCF with the variations of input power, input data rate, mode coupling coefficient and transmission distance are not

performed. From a communication theory perspective, crosstalk due to mode coupling and degradation of system performance (BER) is not seen. To analyze the BER performance of the system, we have calculated the interference crosstalk due to other cores to the centre core and from there we have also evaluated performance indicator SCR and BER for some optimum parameters of optical fiber communication system. Then we have found out few optimal values of coupling coefficient between cores, input power requirement for certain transmission distance, power penalty due to crosstalk and gain of the optical preamplifier needed to compensate the loss.

2.4 Analytical Derivation of Optical Signal Power and Crosstalk Power of the MCF link without Optical Pre-amplifier

Crosstalk and its effect on system performance can be deduced for an optical MCF link in a communication system. The term crosstalk refers to any phenomenon by which a signal transmitted on one circuit or channel of a transmission system creates an undesired effect in another circuit or channel. Crosstalk is usually caused by undesired capacitive, inductive, or conductive coupling from one circuit, part of a circuit, or, channel to another.

However, in an MCF transmission the mode coupling between adjacent cores distorts the signal waveform and limits the transmission performance. The optical crosstalk between adjacent cores is an important problem in an MCF. For a 7 core MCF, interference crosstalk to the centre core due to six outer cores is evaluated by calculating the optical powers at the end of the centre core.

The cores of MCF are spatially positioned such that the field from each core is relatively well isolated and conventional coupled mode theory [24] can be used to analyze the mode coupling dynamics. We assume that each core only supports the LP₀₁ fundamental mode and we denote the amplitude of the LP₀₁ mode of the pth core as $A_p(z)$.

The electric field of the individual core, denoted as $E_p(z)$, can be expressed in terms of its mode amplitude $A_p(z)$ as [26]

$$E_p(z) = A_p(z)e^{-j\beta_p z} \quad (2.18)$$

where β_p represents the propagation constant for the LP₀₁ mode of core p and z is the direction of propagation. The input signal in a homogeneous 7 core MCF is given by

$$\mathbf{E}(0) = [E_1(0) E_2(0) E_3(0) E_4(0) E_5(0) E_6(0) E_7(0)]^H \quad (2.19)$$

and the field at a distance z is given by

$$\mathbf{E}(z) = [E_1(z) E_2(z) E_3(z) E_4(z) E_5(z) E_6(z) E_7(z)]$$

The output at the receiving end of the MCF with length z is given by

$$\mathbf{E}(z) = e^{-\mathbf{R}z} \mathbf{E}(0) \quad (2.20)$$

Where \mathbf{R} contains z independent elements r_{pq} given by

$$r_{pq} = \begin{cases} jC_{pq} & p \neq q \\ j\beta_p & p = q \end{cases} \quad (2.21)$$

from equation (2.21) we get

$$r_{11} = j\beta_1; r_{21} = jC_{21}; r_{31} = jC_{31}; r_{41} = jC_{41}; r_{51} = jC_{51}; r_{61} = jC_{61}; r_{71} = jC_{71}; \quad (2.22)$$

and

$$\mathbf{R} = \begin{bmatrix} r_{11} & \cdots & r_{17} \\ \vdots & \ddots & \vdots \\ r_{71} & \cdots & r_{77} \end{bmatrix}$$

In equation (2.21) C_{pq} is the coupling coefficient (C_k), which is a measure of the spatial overlapping of the mode fields of core p and core q over the cross sectional area of core q. The electric field given by equation (2.20) at a distance z can be expressed as

$$\mathbf{E}(z) = [E_1(z) E_2(z) \dots E_7(z)] = e^{-\mathbf{R}z} [E_1(0) E_2(0) \dots E_7(0)] \quad (2.23)$$

$$= [E_1(0) E_2(0) \dots E_7(0)] \begin{bmatrix} e^{-r_{11}z} & e^{-r_{12}z} & \cdots & e^{-r_{17}z} \\ e^{-r_{21}z} & e^{-r_{22}z} & \cdots & e^{-r_{27}z} \\ \vdots & \vdots & \ddots & \vdots \\ e^{-r_{71}z} & e^{-r_{72}z} & \cdots & e^{-r_{77}z} \end{bmatrix}$$

so,

$$E_1(z) = [E_1(0) E_2(0) \dots E_7(0)] \begin{bmatrix} e^{-r_{11}z} \\ e^{-r_{21}z} \\ \vdots \\ e^{-r_{71}z} \end{bmatrix}$$

$$= E_1(0)e^{-(r_{11}z)} + E_2(0)e^{-(r_{21}z)} \dots E_7(0)e^{-(r_{71}z)} \quad (2.24)$$

Putting value in equation (2.24) from equation (2.22) we get

$$\begin{aligned}
&= E_1(0)e^{-j\beta_1 z} + E_2(0)e^{-jC_{21}z} \dots E_7(0)e^{-jC_{71}z} \quad (2.25) \\
&= E_1(0)\{\cos(\beta_1 z) - j\sin(\beta_1 z)\} + E_2(0)\{\cos(C_{21}z) - j\sin(C_{21}z)\} + \dots \\
&\quad + E_7(0)\{\cos(C_{71}z) - j\sin(C_{71}z)\}
\end{aligned}$$

Separating real and imaginary parts from equation (2.25), we get

$$\begin{aligned}
&E_1(0)\{\cos(\beta_1 z) - j\sin(\beta_1 z)\} + \{E_2(0) \cos(C_{21}z) + E_3(0) \cos(C_{31}z) \dots + \\
&E_7(0) \cos(C_{71}z) - j\{E_2(0) \sin(C_{21}z) + E_3(0) \sin(C_{31}z) + \dots + E_7(0) \sin(C_{71}z)\} \quad (2.26)
\end{aligned}$$

So, when input light signal is given to core 1, i.e. $A_1(0) = 1$, and $A_p(0) = 0$, $p \neq 1$, then from equation (2.26) signal power (P_{sig}) and crosstalk power (P_{CT}) for core 1 can be obtained as under

$$P_{sig}(z) = |E_1(0)|^2 \sqrt{\cos^2(\beta_1 z) + \sin^2(\beta_1 z)}$$

$$\text{or} \quad P_{sig} = |E_1(0)|^2 \quad (2.27)$$

and

$$\begin{aligned}
P_{CT} = &|E_2(0) \cos(C_{21}z) + E_3(0) \cos(C_{31}z) + \dots + E_7(0) \cos(C_{71}z) + E_2(0) \sin(C_{21}z) + \\
&E_3(0) \sin(C_{31}z) + \dots + E_7(0) \sin(C_{71}z)|^2 \quad (2.28)
\end{aligned}$$

$$(SCR)_{optical} = \frac{P_{sig}}{P_{CT}} \quad (2.29)$$

now considering the thermal noise and shot noises at the receiving end, the electrical Signal to Crosstalk plus Noise Ratio (SCNR) can be found by following equation

$$SCNR = \frac{(R_d P_{sig})^2}{2eBI_{CT} + 2eBR_d P_{sig} + \frac{4KT B}{R_L}} \quad (2.30)$$

where $I_{CT} = R_d P_{CT}$ is the crosstalk current and $R_d P_{sig} = I_s$ is the signal current, R_d is the receiver photodiode responsivity, B is the electrical Bandwidth of the receiver, K is the Boltzmann constant, T is the absolute temperature and R_L is the load resistance. Now, for the direct detection system the BER can be evaluated by

$$BER = 0.5 \operatorname{erfc} \frac{\sqrt{SCNR}}{2\sqrt{2}} \quad (2.31)$$

where erfc is the complementary error function.

2.5 Analysis of Electrical SCNR: With Optical Pre-Amplifier

2.5.1 Analysis of Electrical Output Signal and Noises of the MCF Link

The received optical signal with crosstalk at the input of the photodetector at a given distance z from the transmitter is given by

$$e_r(t, z) = \sqrt{2GP_{sig}(z)} e^{j(\omega - \omega_c)t} + \sqrt{2P_{CT}(z)} e^{j((\omega - \omega_c)t - \beta z)} + \sqrt{2P_{ASE}} e^{j\omega t} \quad (2.32)$$

where G is the gain of the optical pre-amplifier and ω and ω_c are the angular frequency and optical carrier frequency.

The photo current at the output of the photo detector can be expressed as:

$$\begin{aligned} i_d(t, z) &= R_d \cdot E |Re \{e_r(t, z)\}|^2 \quad (2.33) \\ &= R_d \cdot E |Re \{\sqrt{2GP_{sig}(z)} e^{j(\omega - \omega_c)t} + \sqrt{2P_{CT}(z)} e^{j((\omega - \omega_c)t - \beta z)} + \sqrt{2P_{ASE}} e^{j\omega t}\}|^2 \\ &= R_d \cdot E |\sqrt{2GP_{sig}(z)} \cos(\omega - \omega_c)t + \sqrt{2P_{CT}(z)} \cos((\omega - \omega_c)t - \beta z) + \\ &\quad \sqrt{2P_{ASE}} \cos \omega t|^2 \\ &= R_d \cdot P_{sig}(z) \cdot G + R_d \cdot P_{CT}(z) + R_d \cdot P_{ASE} + 2R_d \sqrt{P_{sig}(z) \cdot P_{CT}(z) \cdot \cos \beta z} + \\ &\quad 2R_d \sqrt{P_{sig}(z) \cdot P_{ASE} \cdot \cos(\omega - \omega_c)t} + 2R_d \sqrt{P_{CT}(z) \cdot P_{ASE} \cdot \cos(\omega - \omega_c)t} \\ &= I_{sig} \cdot G + I_{CT}(t) + I_{ASE}(t) + I_{shot}(t) + I_{sig-CT}(t) + I_{sig-ASE}(t) + I_{CT-ASE}(t) \end{aligned}$$

The pre-amplifier is followed by photo detector and the current at the output of pre amplifier is given by

$$\begin{aligned} I_o(t) &= I_{sig}(z) \cdot G + I_{CT}(t) + I_{ASE}(t) + I_{shot}(t) + I_{sig-CT}(t) + I_{sig-ASE}(t) \\ &\quad + I_{CT-ASE}(t) + I_{th}(t) \end{aligned}$$

where $I_{th}(t)$ is the thermal noise due to pre-amplifier.

The variances of the noise component in the detector and the pre-amplifier can be summarized as

$$\sigma_{shot}^2 = 2eB (R_d \cdot G \cdot P_{sig} + R_d \cdot P_{CT} + R_d \cdot P_{ASE}) \quad (2.34)$$

$$\sigma_{CT}^2 = (R_d \cdot P_{CT})^2$$

$$P_{ASE} = \sigma_{ASE}^2 = n_{sp} (G - 1) h \gamma \cdot B_0$$

$$\begin{aligned}\sigma_{sig-CT}^2 &= 4R_d^2 \cdot P_{sig} \cdot P_{CT} \cdot \cos^2 \beta z \\ \sigma_{sig-ASE}^2 &= 2R_d^2 \cdot P_{sig} \cdot [n_{sp}(G-1)h\gamma \cdot B_0] \\ \sigma_{CT-ASE}^2 &= 2R_d^2 \cdot P_{CT} \cdot [n_{sp}(G-1)h\gamma \cdot B_0] \\ \sigma_{th}^2 &= \frac{4KT}{R_l} \cdot B\end{aligned}$$

where B_0 is the bandwidth of optical amplifier.

Then considering the total variances, the electrical signal to crosstalk plus noise ratio at the output of low pass filter is given by

$$eSCNR = \frac{I_{sig}^2 \cdot G^2}{\sigma_{shot}^2 + \sigma_{CT}^2 + \sigma_{ASE}^2 + \sigma_{sig-CT}^2 + \sigma_{sig-ASE}^2 + \sigma_{CT-ASE}^2 + \sigma_{th}^2} \quad (2.35)$$

2.6 Bit Error Rate Analysis

In digital optical communications, BER is defined as the ratio of bits in error to total number of transmitted bit at the decision point, is commonly used as a figure of merit. For an intensity modulated signal, the output current may have two average values corresponding to the bit “1” or “0”. Bit error occurs when a “1” is received as a “0” or “0” is received as a “1”. If $P(1)$ and $P(0)$ are the probabilities of transmission for binary ones and zeros, respectively, then the total probability of error $P(e)$ may be defined as:

$$P(e) = P(1)P(0|1) + P(0)P(1|0) \quad (2.35)$$

where $P(0|1)$ is the probability that a “0” is received when a “1” is transmitted and $P(1|0)$ is the probability that a “1” is received when a “0” is transmitted. If we assume that a binary code is chosen such that the number of transmitted ones and zeros is equal, then $P(0) = P(1) = 1/2$, and the net probability of error is one-half then equation. (2.35) becomes:

$$P(e) = 1/2 [P(0|1) + P(1|0)] \quad (2.36)$$

The BER is the key figure of merit in an optical fiber communications system and must be accurately calculated when designing systems [30]. For a system researcher, it poses a real challenge as the transmission errors are caused by a large number of phenomena, both deterministic and stochastic in nature. In this work, we have addressed one

important aspect of the BER evaluation, the effect of coupling coefficient of mode power on transmission of optical signals and its contribution to the BER along with the noise from optical amplifiers.

In this paper, we studied the effect of crosstalk due to mode power coupling from adjacent cores of MCF and BER generated from this phenomena. BER is acceptable upto certain limit for different types of transmission (voice, data video etc). So measurement of BER is very important. Considering all the noises discussed so far and for a modulation schemes of on-off keying (OOK) signal the system performance (BER) can be measured by

$$\text{BER} = 0.5 \operatorname{erfc} \frac{\sqrt{eSCNR}}{2\sqrt{2}} \quad (2.37)$$

CHAPTER 3

RESULTS AND DISCUSSION

3.1 Introduction

Following the analytical formulation presented in chapter 2, we evaluate the performance of an optical communication system with MCF as the transmission waveguide. The results are evaluated in terms of optical signal power and crosstalk power, optical signal to crosstalk ratio (SCR) at the output of the MCF. The electrical Signal to Crosstalk plus Noise Ratio (SCNR) and BER at the output of a direct detection receiver are also evaluated for different fiber and system parameters. The parameters used for numerical computations are shown in Table 3.1 below.

Table 3.1 Parameters for Numerical Computations

Parameter	Symbol	Value
Wavelength	λ	1550 nm
Coupling Coefficient	K_c	0.5 - 2.5
Input Power	P_{in}	-3 dBm to 1 dBm -10 dBm to -5 dBm -20 dBm to -15 dBm
Number of Cores	p	7
Refractive Index		
Core	n_1	1.51
Cladding	n_2	1.44
Data rate	R_b	1 Gbps- 10 Gbps
Gain	G	20 dB
Core Diameter	'2a'	8 μ m
Cladding diameter	'd'	125 μ m
Core to Core pitch	Δ	30 μ m
Distance	z	100 m and 1 km

3.2 Performance Results without Optical Pre-Amplifier

3.2.1 Evaluation of SCNR

Using the appropriate parameter values we compute the signal power in core 1 received at the output of MCF (at the input to the receiver) for different values of the input optical power. The crosstalk plus the noise power coupled to core 1 from other six cores is also evaluated. The electrical signal to noise plus crosstalk ratio (SCNR) is then evaluated at the output of the direct detection receiver. The plots of SCNR versus transmission distance z are shown in Fig 3.1 and Fig. 3.2 with input power as a parameter at data rates of 2.5 Gbps and 10 Gbps respectively with coupling coefficient, $K_c = 0.5$. It is noticed that the SCNR decreases with the increase of transmission distance due to fiber loss. From both the figures it is also noticed that transmission distance increases with the increase in input power for a given output SCNR. Further, there is a loss in SCNR at higher data rates due to higher amount of crosstalk and noise at higher bandwidth.

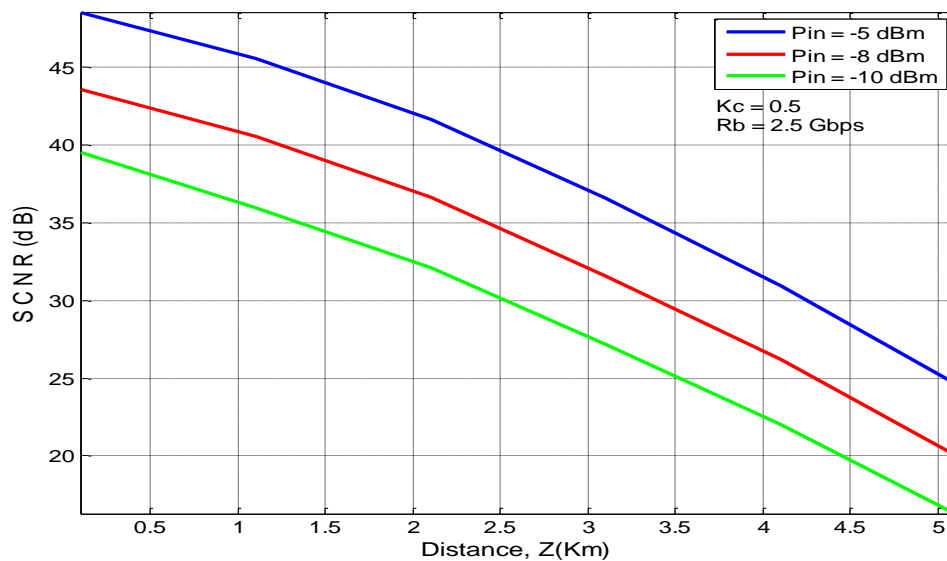


Fig. 3.1 Plots of SCNR at the output of a 7 core MCF as a function of distance with input optical power, $P_{in} = -5$ dBm, -8 dBm and -10 dBm and coupling coefficient $K_c = 0.5$, data rate, $R_b = 2.5$ Gbps

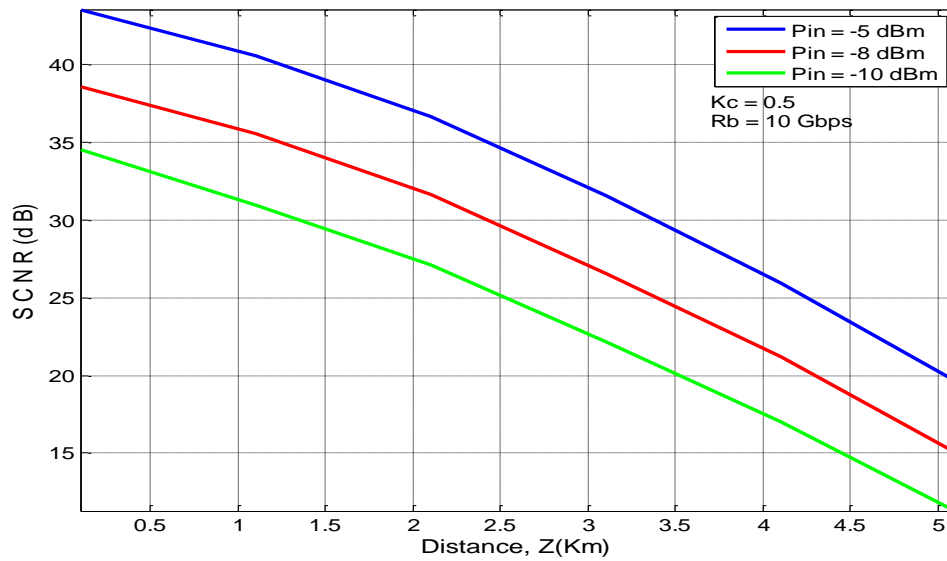


Fig. 3.2 Plots of SCNR at the output of a 7 core MCF as a function of distance with input optical power, $P_{in} = -5$ dBm, -8 dBm and -10 dBm and coupling coefficient $K_c = 0.5$, data rate, $R_b = 10$ Gbps

3.2.2 Effect of BER on Transmission Distance

The plots of BER versus transmission distance z are shown in Fig. 3.3(a), Fig. 3.3(b) and Fig. 3.3(c) for different input optical power, $P_{in} = -20$ dBm, -18 dBm and -15 dBm and data rate of 1 Gbps, 2.5 Gbps and 10 Gbps respectively. It is noticed that there is increase in BER with the increase in transmission distance which is due to decrease in SCNR caused by increase in crosstalk. It is also observed that allowable transmission distance is less for higher data rate. For example the allowable transmission distance corresponding to BER 10^{-9} are found to be 5.5 Km, 4.9 km and 3.7 Km for 1 Gbps, 2.5 Gbps and 10 Gbps data rate respectively for -15 dBm power input (Fig. 3.3 (c)). From comparison of the Fig. 3.3(a), 3.3(b) and 3.3(c) it is also observed that for a given BER (say 10^{-9}) there is increase in the allowable transmission distance with the increase in input optical power level.

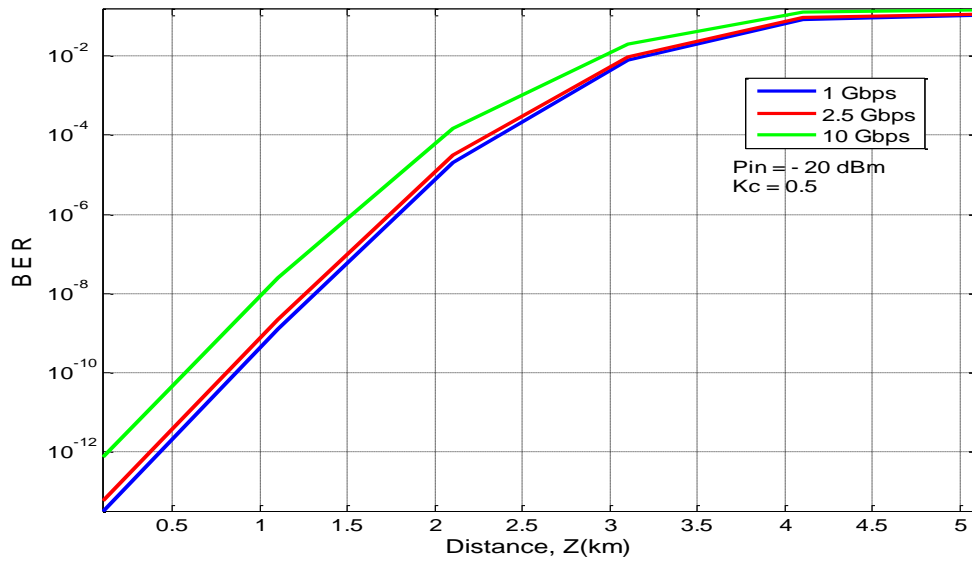


Fig. 3.3(a) Plots of BER of a direct detection optical link with a 7 core MCF as a function of distance with input optical power, $P_{in} = -20$ dBm for three different data rate of $R_b = 1$ Gbps, 2.5 Gbps and 10 Gbps and coupling coefficient, $K_c = 0.5$

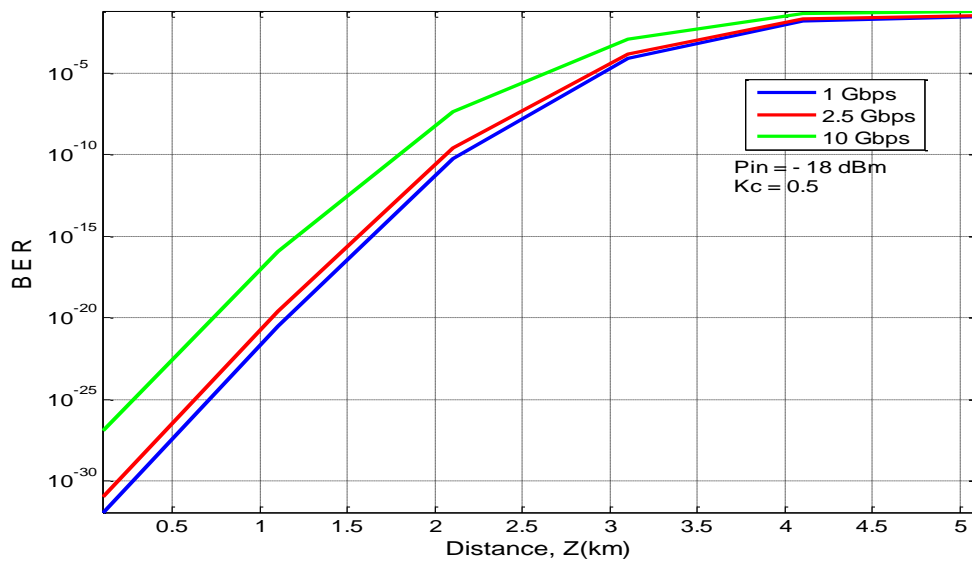


Fig. 3.3(b) Plots of BER of a direct detection optical link with a 7 core MCF as a function of distance with input optical power, $P_{in} = -18$ dBm for three different data rate of $R_b = 1$ Gbps, 2.5 Gbps and 10 Gbps and coupling coefficient, $K_c = 0.5$

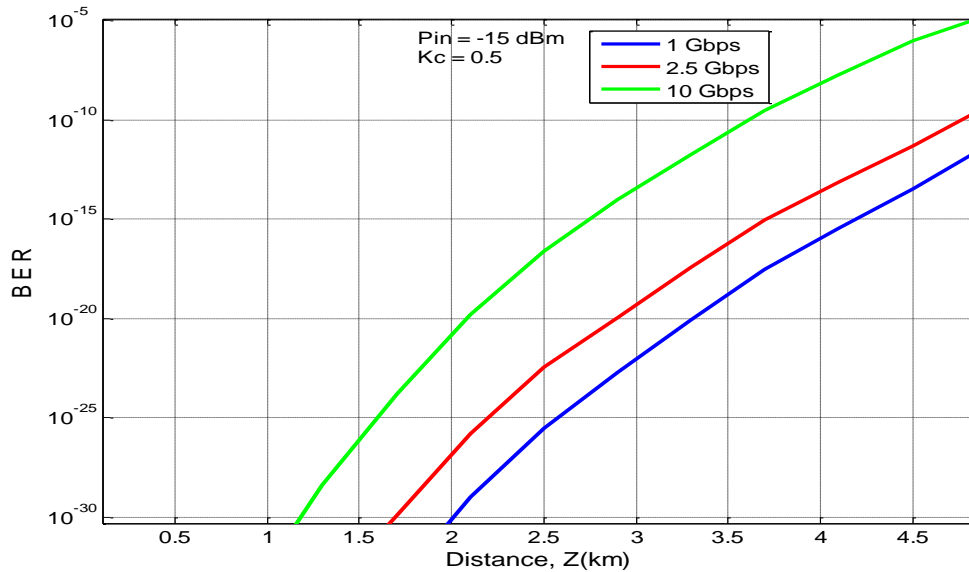


Fig 3.3(c) Plots of BER of a direct detection optical link with a 7 core MCF as a function of distance with input optical power, $P_{in} = -15$ dBm for three different data rate of $R_b = 1$ Gbps, 2.5 Gbps and 10 Gbps and coupling coefficient, $K_c = 0.5$

3.2.3 Effect of Coupling Co-efficient on SCNR

The effect of coupling co-efficient on SCNR are shown in figure 3.4(a), 3.4(b) and 3.4(c) for three different data rates of 1 Gbps, 2.5 Gbps and 10 Gbps respectively. From Fig. 3.4(a) it is seen that there is significant reduction in SCNR due to increased crosstalk with the increase of coupling co-efficient. For example in Fig. 3.4(a) at 100 m distance the SCNR is 78 dB at $K_c = 0.5$ but at same distance SCNR is 44 dB for $K_c = 1.0$. Again it is seen that the SCNR decreases with the increase of distance for the same Coupling co-efficient. For example from Fig. 3.4(b) the SCNR are found to be 17 dB and 6 dB at coupling co-efficients of 1.0 at distance of 100 m and 1 Km respectively. Comparison of figures reveals that there is significant reduction in SCNR with increase in data rates. For example from Fig 3.4(b) and Fig. 3.4(c) the SCNR are found to be 17 dB and 7 dB respectively for 100 m distance at $K_c = 1.0$.

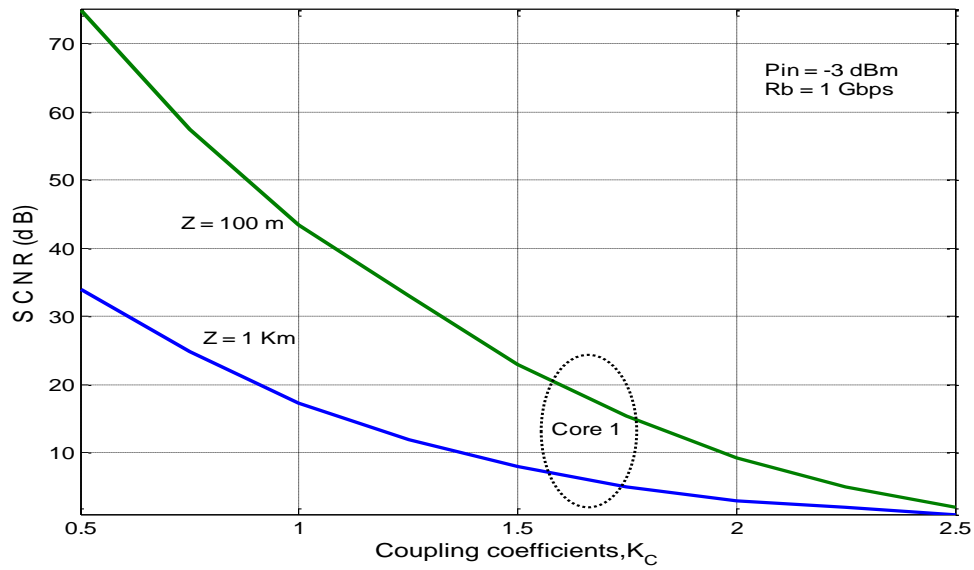


Fig. 3.4(a) Plots of SCNR at the output of a 7 core MCF as a function of Coupling Coefficient of ranges, $K_c = 0.5- 2.5$ with input optical power, $P_{in} = -3$ dB, data rate, $R_b = 1$ Gbps, for two separate distance, $Z = 100$ m and $Z = 1$ km

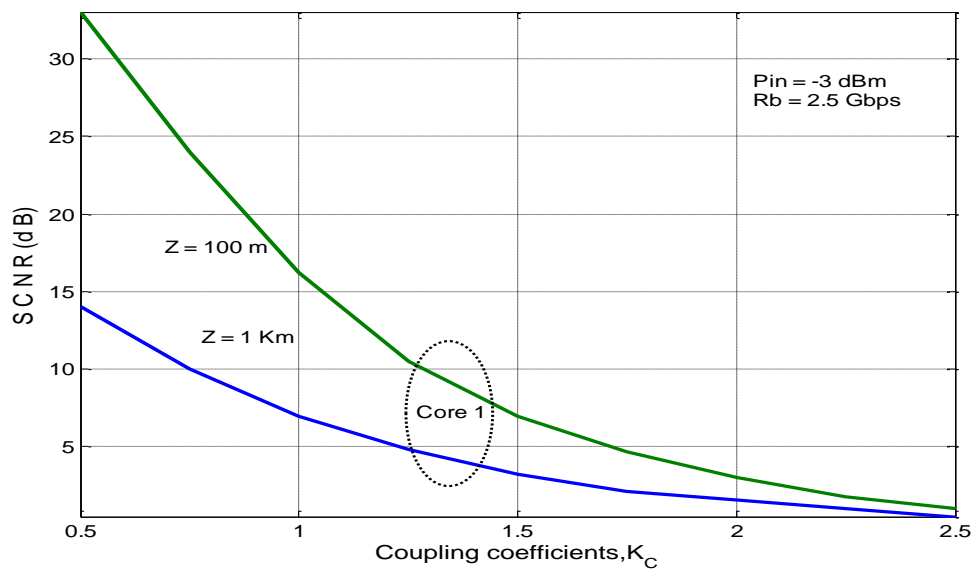


Fig. 3.4(b) Plots of SCNR at the output of a 7 core MCF as a function of Coupling Coefficient of ranges, $K_c = 0.5- 2.5$ with input optical power, $P_{in} = -3$ dB, data rate, $R_b = 2.5$ Gbps, for two separate distance, $Z = 100$ m and $Z = 1$ km

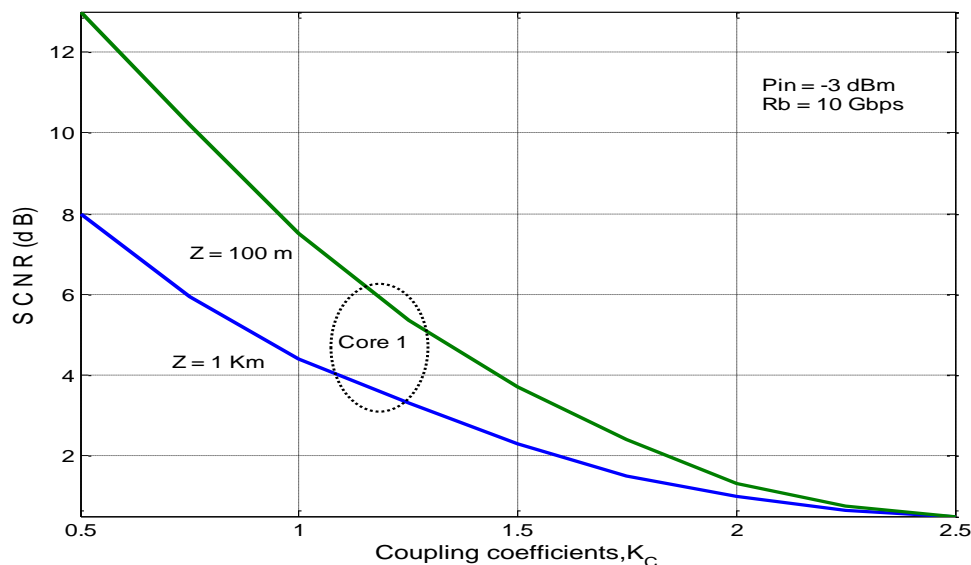


Fig. 3.4(c) Plots of SCNR at the output of a 7 core MCF as a function of Coupling Coefficient, $K_c = 0.5- 2.5$ with input optical power, $P_{in} = -3$ dB, data rate, $R_b = 10$ Gbps, for two separate distance, $Z = 100$ m and $Z = 1$ km

3.2.4 Effect of Coupling Co-efficient on BER

Coupling co-efficient, K_c is very important in mode coupling dynamics. Plots of BER against Coupling co-efficient are shown in Fig 3.5(a), 3.5(b) and 3.5(c) for three different data rate and for two separate transmission distance. It is seen that with the increase of coupling co-efficient the BER increases due to higher crosstalk. It is also noticed that for a BER(10^{-9}) the coupling co-efficient is reduced to increase the transmission distance. For example to keep the BER at 10^{-9} for 1 Gbps data rate, the coupling co-efficient has to be reduced to 1.18 for 1 km of distance, where as it could be 1.5 for 100 m transmission distance. It is further noticed that for higher data rate the coupling co-efficient has to be lowered to attain the same BER of 10^{-9} . For example, at 2.5 Gbps of data rate the allowable coupling co-efficients can be maximum 0.65 and 1.18 for the distance of 1km and 100 m respectively. It is also noticed that to maintain a standard output power level and to keep the coupling co-efficient constant the input power in the core may have to be increased. For example in Fig. 3.5(b) and in Fig. 3.5(c) the input power is increased to -1 dBm and 1 dBm respectively.

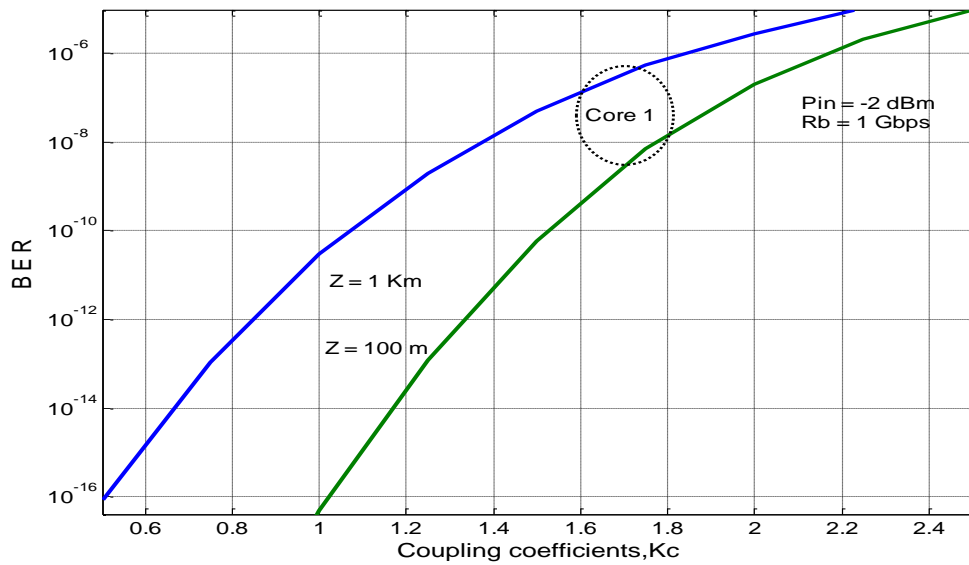


Fig. 3.5(a) Plots of BER at the output of a 7 core MCF as a function of Coupling Coefficient, $K_c = 0.5- 2.5$ with input optical power, $P_{in} = -2 \text{ dBm}$, data rate of $R_b = 1 \text{ Gbps}$ and for two separate distance of $Z = 100 \text{ m}$ and $Z = 1 \text{ km}$

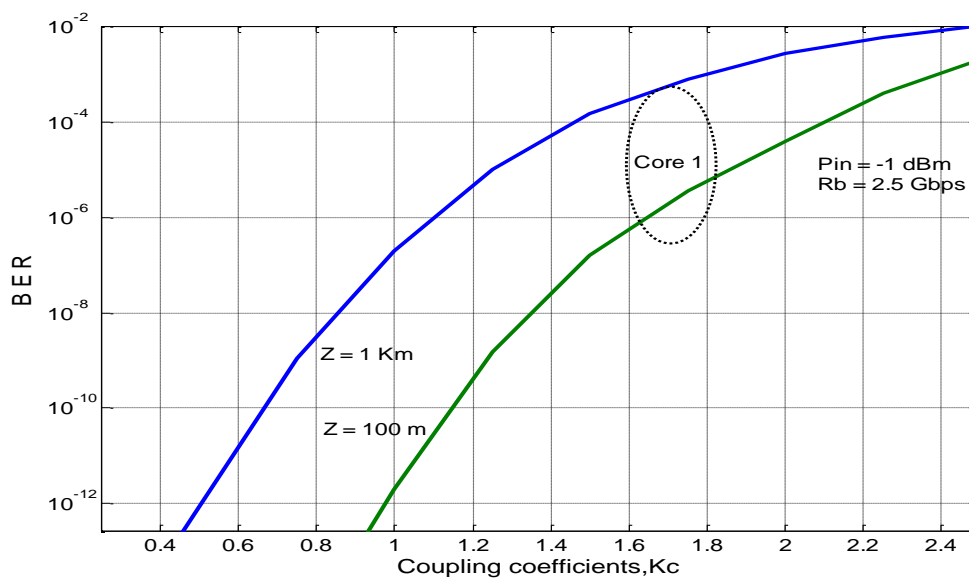


Fig. 3.5(b) Plots of BER at the output of a 7 core MCF as a function of Coupling Coefficient, $K_c = 0.5- 2.5$ with input optical power, $P_{in} = -1 \text{ dBm}$, data rate of $R_b = 2.5 \text{ Gbps}$ and for two separate distance of $Z = 100 \text{ m}$ and $Z = 1 \text{ km}$

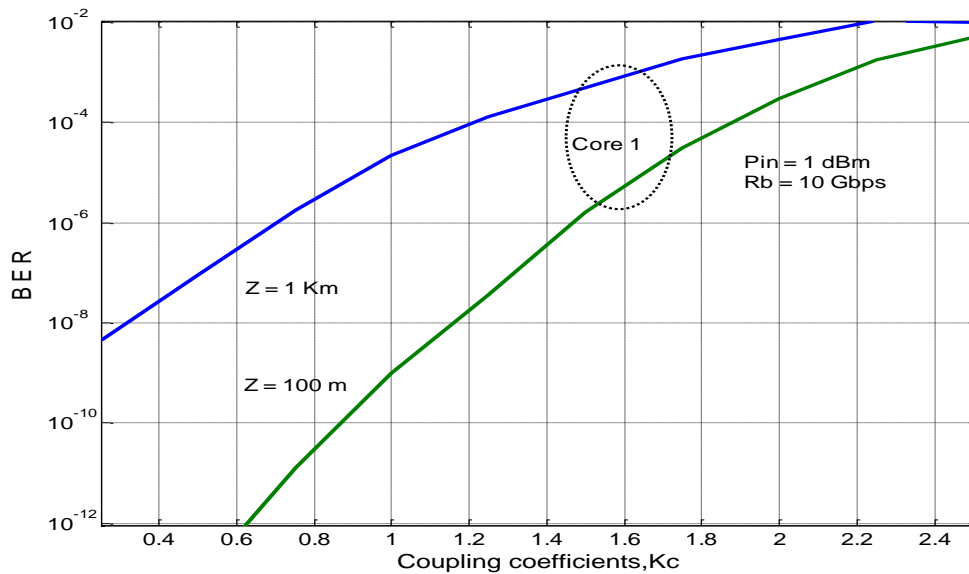


Fig. 3.5(c) Plots of BER at the output of a 7 core MCF as a function of Coupling Coefficient, $K_c = 0.5- 2.5$ with input optical power, $P_{in} = 1 \text{ dBm}$, data rate of $R_b = 10 \text{ Gbps}$ and for two separate distance of $Z = 100 \text{ m}$ and $Z = 1 \text{ km}$

3.2.5 Effect of SCNR over BER

The Effect of electrical SCNR over BER is shown in Fig. 3.6(a), 3.6(b) and 3.6(c) for three different data rates of 1 Gbps, 2.5 Gbps and 10 Gbps and for a range of coupling co-efficient of 0.5-2.5. It is seen that with the increase of SCNR the BER decreases. For example for 10 Gbps data rate, at $K_c = 1.5$, for $\text{SCNR} = 31.62 \text{ dB}$ the BER is 1×10^{-9} , where as for $\text{SCNR} = 32.3 \text{ dB}$ the BER is reduced to 3×10^{-10} while keeping other parameters unchanged. It is further noticed that there is increase of input power power due to increase of data rate. That is to keep the BER at the specified level (10^{-9}) the input power has to be increased. For example, in the Fig. 3.6(a), 3.6(b) and 3.6(c) the input power required is used are 4.5 dBm, 6.5 dBm and 9.5 dBm for 1 Gbps, 2.5 Gbps and 10 Gbps respectively to keep the BER at 10^{-9} . Thus the system suffers power penalty due to crosstalk at agiven BER.

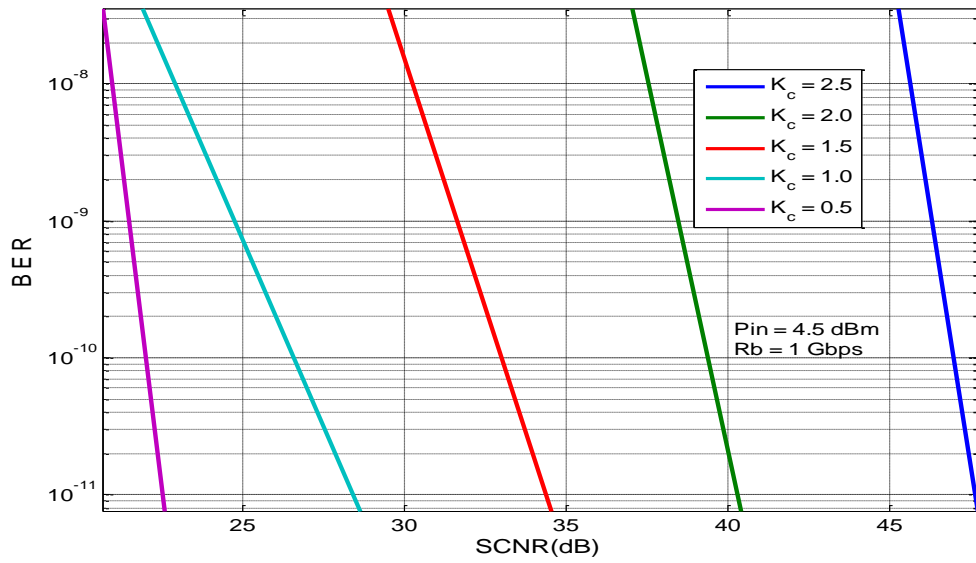


Fig 3.6(a) Plots of BER at the output of a 7 core MCF as a function of SCNR with input optical power, $P_{in} = 4.5$ dBm for data rate of $R_b = 1$ Gbps

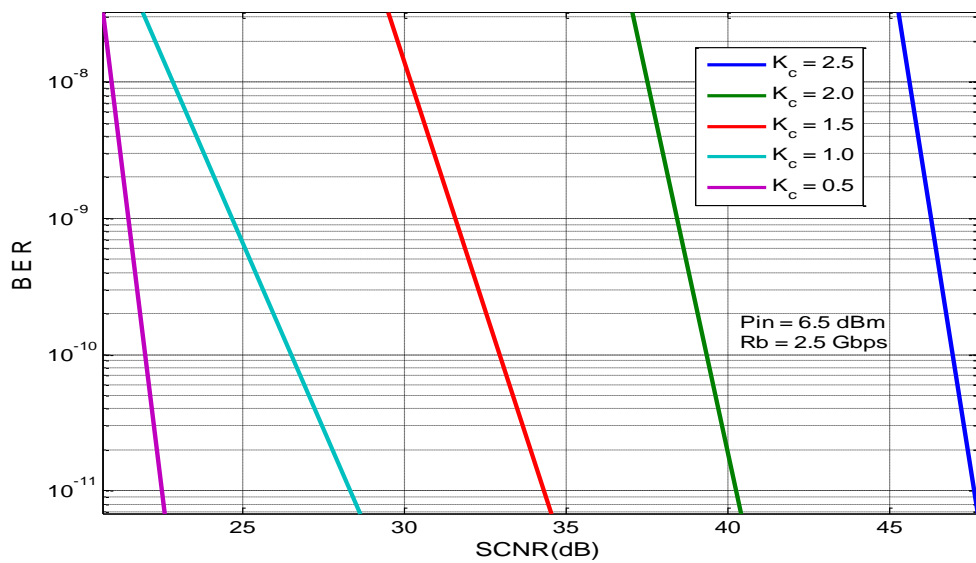


Fig 3.6(b) Plots of BER at the output of a 7 core MCF as a function of SCNR with input optical power, $P_{in} = 6.5$ dBm for data rate of $R_b = 2.5$ Gbps

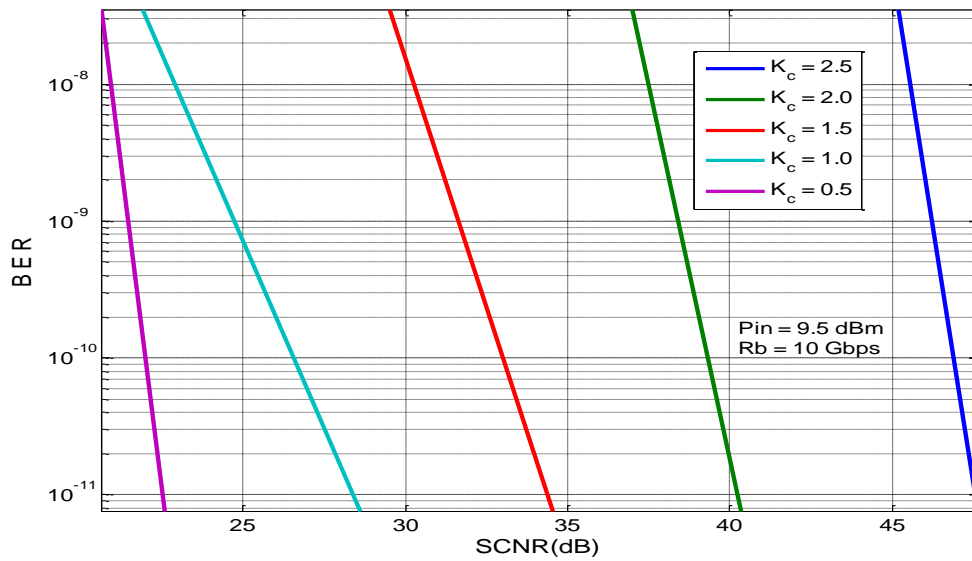


Fig. 3.6(c) Plots of BER at the output of a 7 core MCF as a function of SCNR with input optical power, $P_{in} = 9.5$ dBm for data rate of $R_b = 10$ Gbps

3.2.6 Effect of Coupling Co-efficient on Power Penalty

In Fig. 3.7, the power penalty at a BER of 10^{-9} is plotted as a function of the coupling co-efficient. It is found that power penalty increases with coupling coefficient. For example at coupling co-efficient, $K_c = 0.8$, the power penalty are 3.40 dB, 4.20 dB and 4.88 dB respectively for data rates of 1 Gbps, 2.5 Gbps and 10 Gbps, but at coupling co-efficient, $K_c = 1.0$, the power penalty are 4.50 dB, 5.50 dB and 6.40 dB respectively for data rates of 1 Gbps, 2.5 Gbps and 10 Gbps.

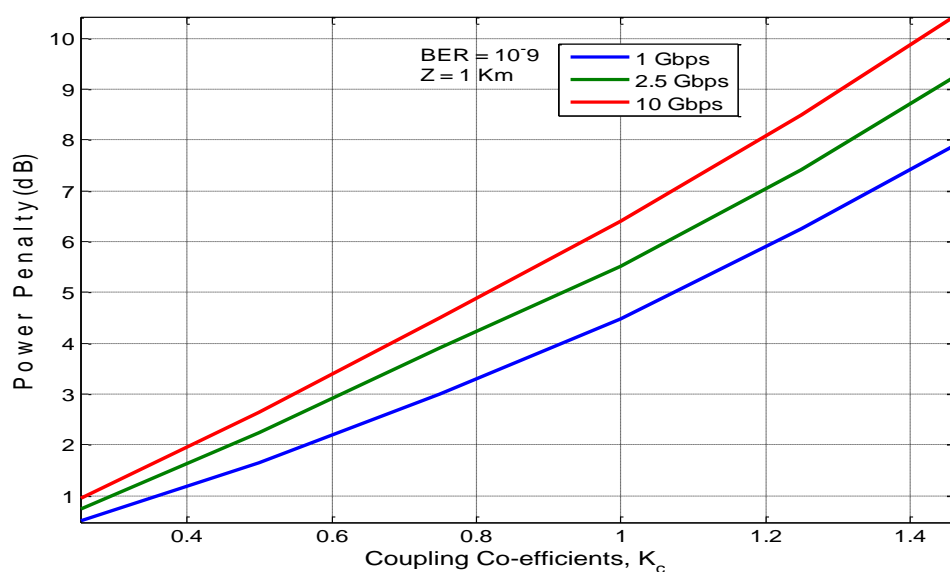


Fig. 3.7 Plots of Power Penalty(dB) as a function of Coupling co-efficient for different data rates and at transmission distance $Z = 1$ km.

3.2.7 Effect of Input Power on Transmission Distance

In Fig. 3.8, the transmission distance is plotted as a function of input Power. It is found that input power requirement is high for higher transmission distance. For a given input power and for a required BER (10^{-9}) allowable transmission distance can be found from the plot. For example at input power of -18.5 dBm, maximum allowable transmission distance for 1 Gbps, 2.5 Gbps and 10 Gbps data rates are respectively 3.10 km, 2.65 km and 1.52 km. So, it is found that low data rate allows more transmission distance.

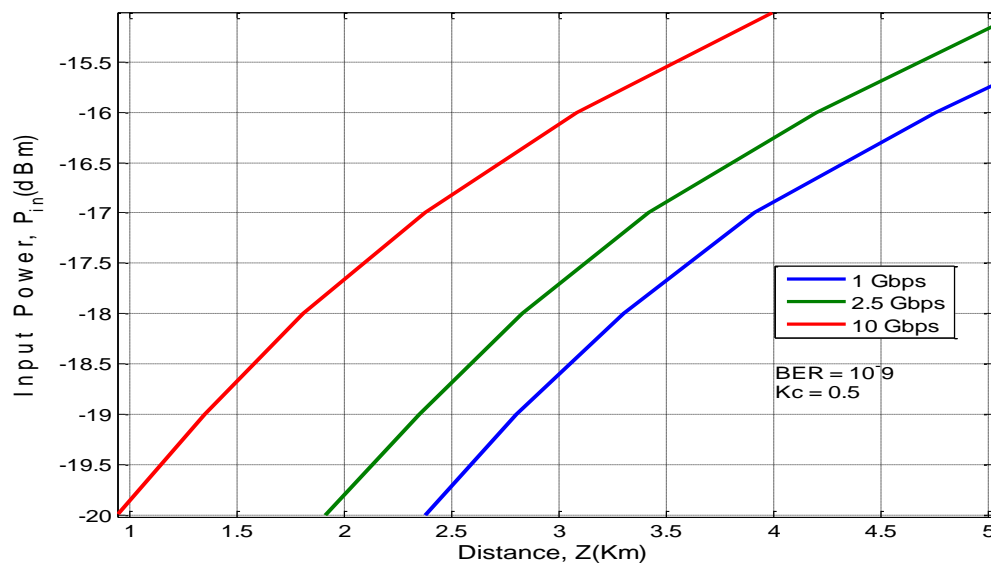


Fig. 3.8 Plots of transmission distance as a function of input optical power for different data rates.

3.3 Performance Results with Optical Pre-Amplifier

3.3.1 Effect of Electrical SCNR on Transmission Distance

Following the analytical formulation presented in paragraph 2.3, we evaluate the performance of an optical MCF communication system with an optical pre-amplifier. Using the appropriate parameter values we compute the SCNR at the output of the direct detection receiver. The plots of SCNR versus transmission distance z are shown in Fig. 3.9(a) and in Fig. 3.9(b). It is noticed that the SCNR decreases with the transmission distance. The transmission distance increases with the increase of input power. From comparison of Fig. 3.9(a) and Fig. 3.9(b) it is noticed that SCNR is reduced with increase in coupling co-efficient.

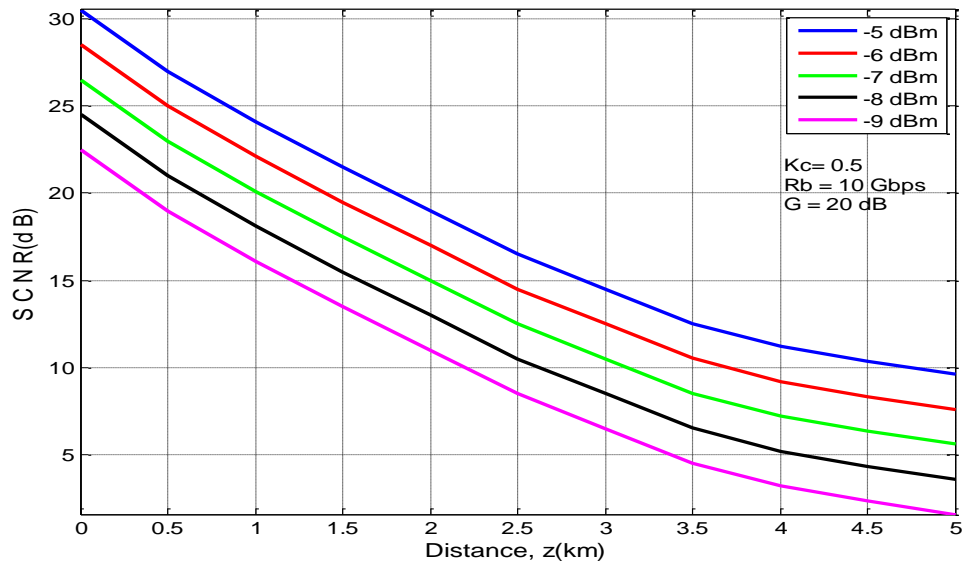


Fig. 3.9(a) Plots of SCNR (dB) as a function of link distance with different input optical power, at a data rate of $R_b = 10$ Gbps, $K_c = 0.5$ and $G = 20$ dB

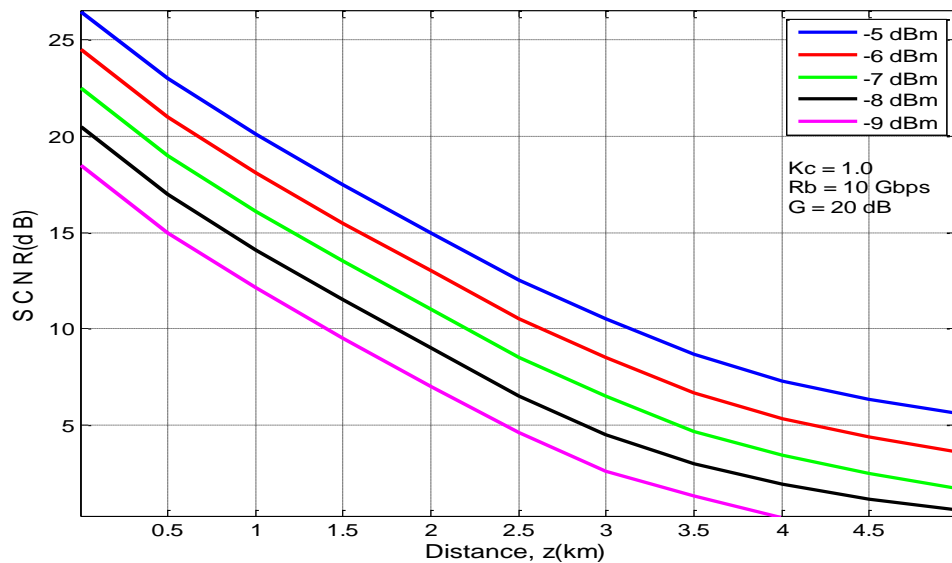


Fig. 3.9(b) Plots of SCNR (dB) as a function of link distance with different input optical power, at a data rate of $R_b = 10$ Gbps, $K_c = 1.0$ and $G = 20$ dB

3.3.2. Effect of BER on Transmission Distance

The plots of BER versus transmission distance z are shown in Fig. 3.10(a) and Fig. 3.10(b). It is noticed that there is increase in BER with the increase of transmission distance. It is also observed that allowable transmission distance is less for higher coupling coefficient. For example, the allowable transmission distance for BER 10^{-9} are found to be 2.55 km for input power, of $P_{in} = -9$ dBm for coupling coefficient, $K_c = 0.5$, whereas it is only 2.40 km for coupling coefficients, $K_c = 1.0$. So, it can be understood

that with the increase of coupling coefficient the crosstalk increases, which ultimately limits the transmission distance of the link.

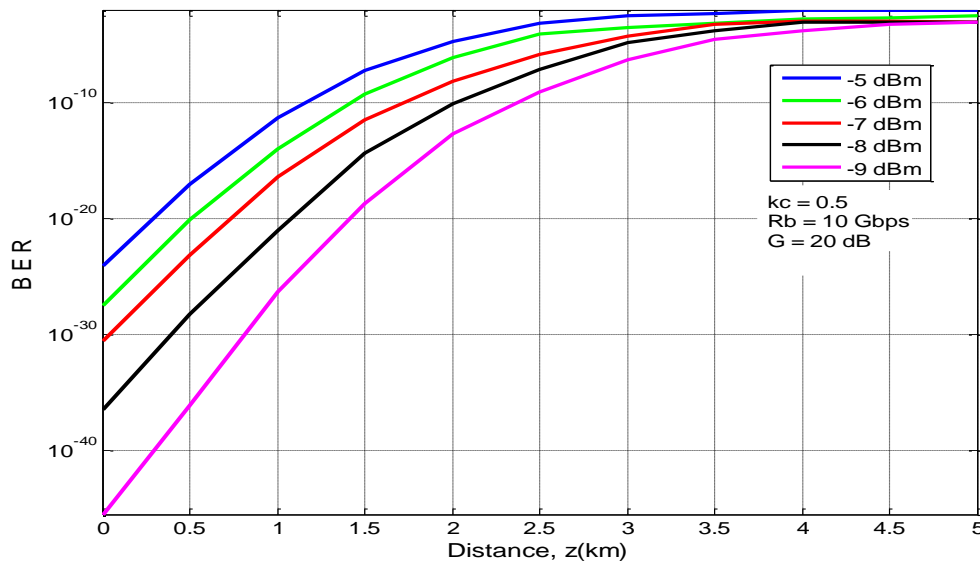


Fig. 3.10(a) Plots of BER as a function of link distance with different input power, at a data rate of $R_b = 10$ Gbps, $K_c = 0.5$ and $G = 20$ dB

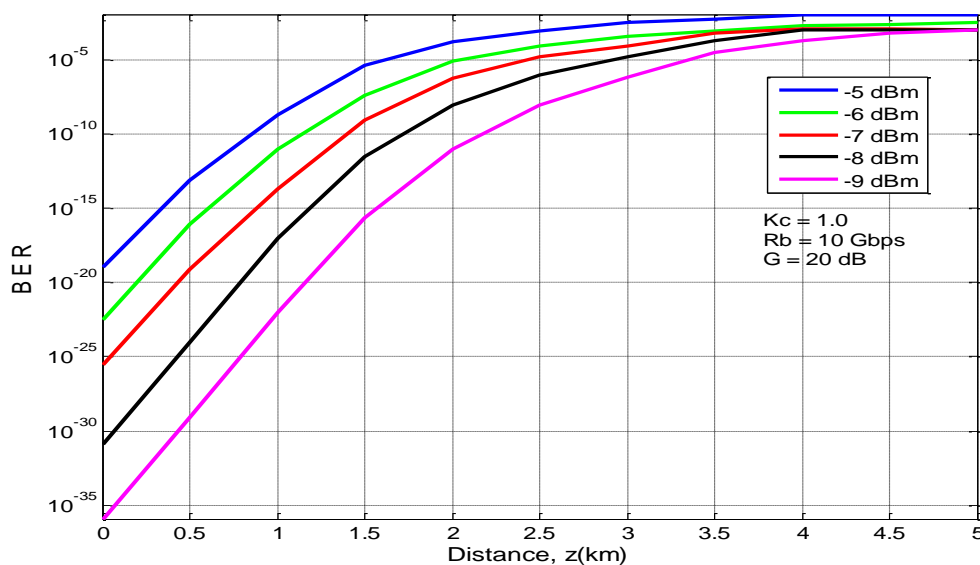


Fig. 3.10(b). Plots of BER as a function of link distance with different input power, at a data rate of $R_b = 10$ Gbps, $K_c = 1.0$ and $G = 20$ dB

3.3.3 Effect of Input Power on Transmission Distance

In Fig. 3.11 allowable transmission distance of the system at $BER = 10^{-9}$ is plotted as a function of input power. It is seen that with the increase in input power level the link distance increases. Again it is observed that for different data rate the change is not that significant. It is due to the fact that optical crosstalk power is a function of coupling coefficient rather than bandwidth.

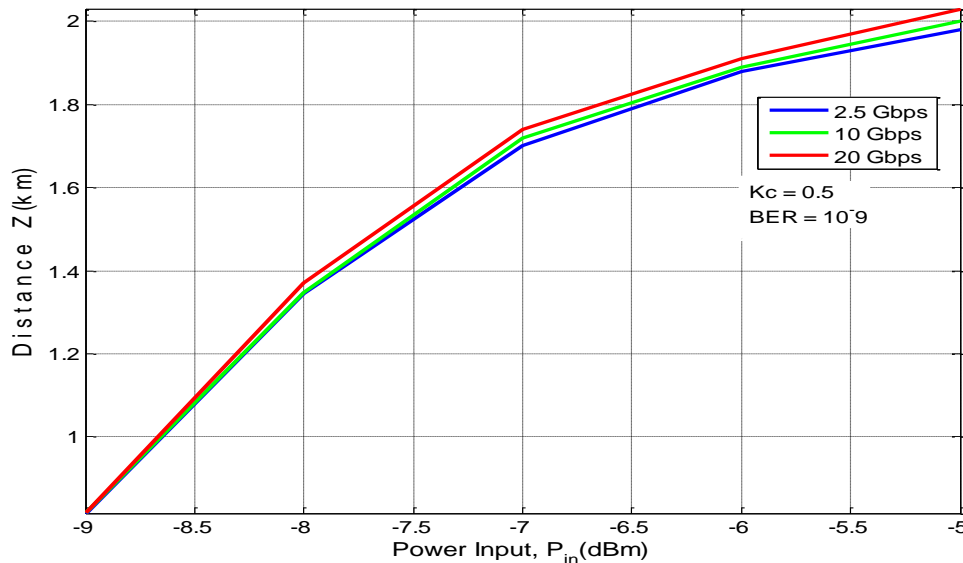


Fig. 3.11 Plots of Transmission distance as a function of power input for different data rate and coupling coefficient, $K_c = 0.5$

3.3.4 Effect of Coupling Co-efficient on SCNR

In Fig. 3.12 SCNR is plotted as a function of coupling coefficient. It is seen that with the increase of coupling coefficient the SCNR decreases. Again it is noticed that with increase of power input the SCNR increases. So, it can be said that to compensate the crosstalk due to coupling coefficient, increasing the input power level is one of the option. For -15 dBm input power the SCNR falls to zero at $K_c = 2.35$ and above. For a short span of link this is acceptable, but for medium and long distances K_c should be less than 2.35.

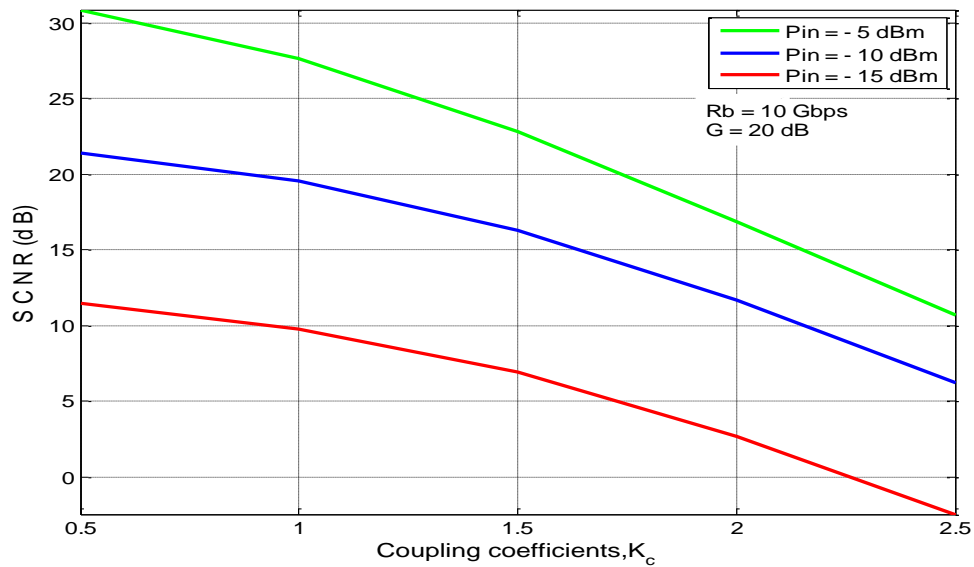


Fig. 3.12 Plots of SCNR (dB) as a function of coupling coefficient for different power input, and $G = 20$ dB

3.3.5. Effect of Coupling Coefficients on BER

In Fig. 3.13 BER is plotted as a function of coupling coefficient. It is observed that with the increase of coupling coefficient the BER increases. It is further noticed that as the input power level increases the BER decreases. So to keep the BER at an acceptable margin (10^{-9}), the input power needs to be increased. It is noticed that to maintain a standard BER (10^{-9}), allowable coupling coefficient for input power of -10 dBm, -7 dBm and -5 dBm, the maximum coupling coefficient can be $K_c = 0.7$, $K_c = 1.65$ and $K_c = 1.85$ respectively.

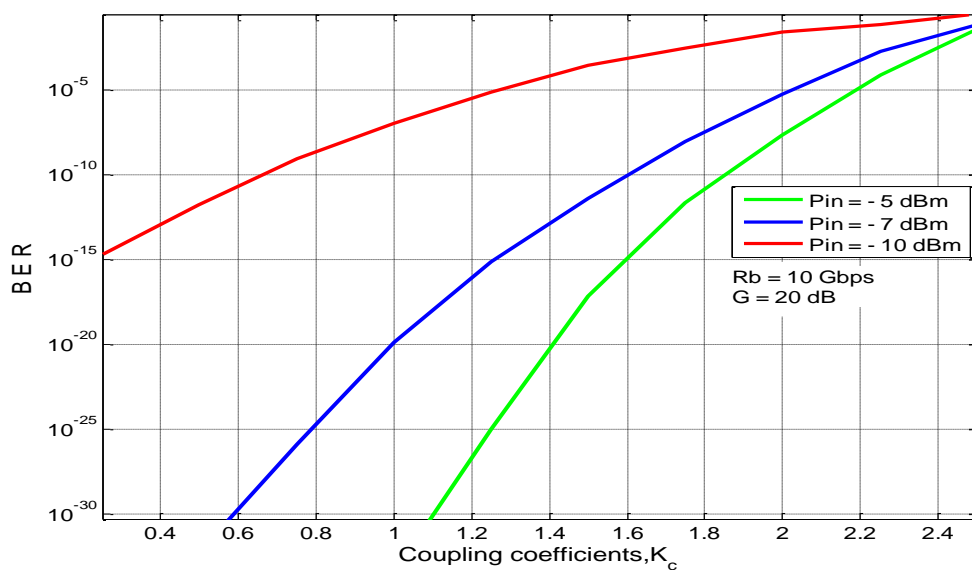


Fig. 3.13 Plots of BER as a function of link distance for different input power, $R_b = 10$ Gbps and $G = 20$ dB.

3.3.6 Effect of Optical Pre-Amplifier Gain on SCNR

In Fig. 3.14 the SCNR is plotted as a function of transmission distance with varying gain level of the pre-amplifier. It is marked that SCNR decreases with the link distance, but to keep the SCNR at a fixed level the gain of the pre-amplifier should be increased or adjusted.

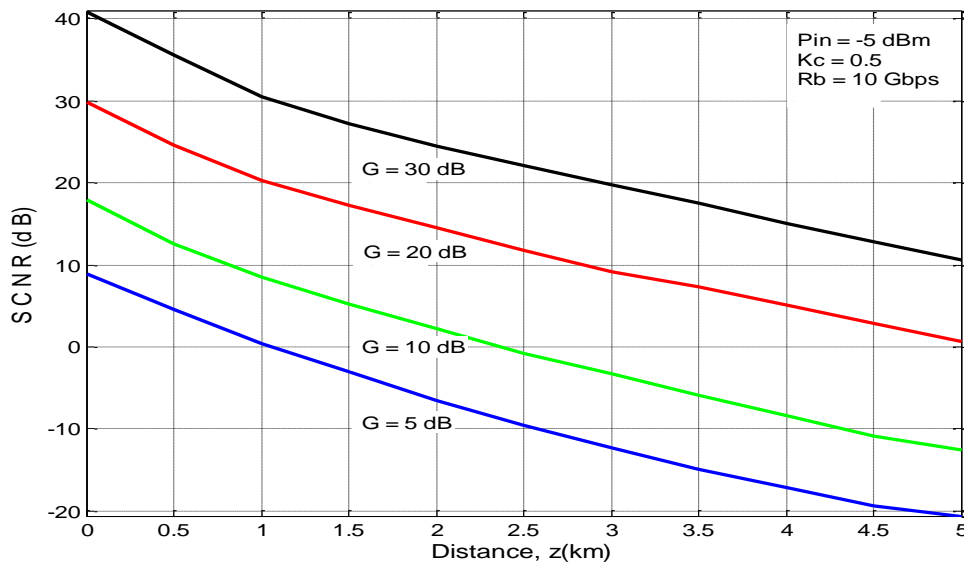


Fig. 3.14 Plots of SCNR (dB) as a function of link distance for different gain (G) level, $R_b = 10$ Gbps, $P_{in} = -5$ dBm and $K_c = 0.5$

3.3.7 Effect of Optical Pre-Amplifier Gain on BER

In Fig. 3.15 BER is plotted as a function of distance. It is seen that BER increases with the increases of distance, but to keep the BER at an acceptable level, i.e. 10^{-9} , gain of the pre-amplifier should be adjusted. For this system it is seen that to achieve minimum BER of 10^{-9} at least 15 dB gain is required. Again it noticed that, to attain certain distance, specific gain is required to compensate the crosstalk. For example, to reach a distance of 3.8 km with BER 10^{-9} , at least 25 dB gain is needed.

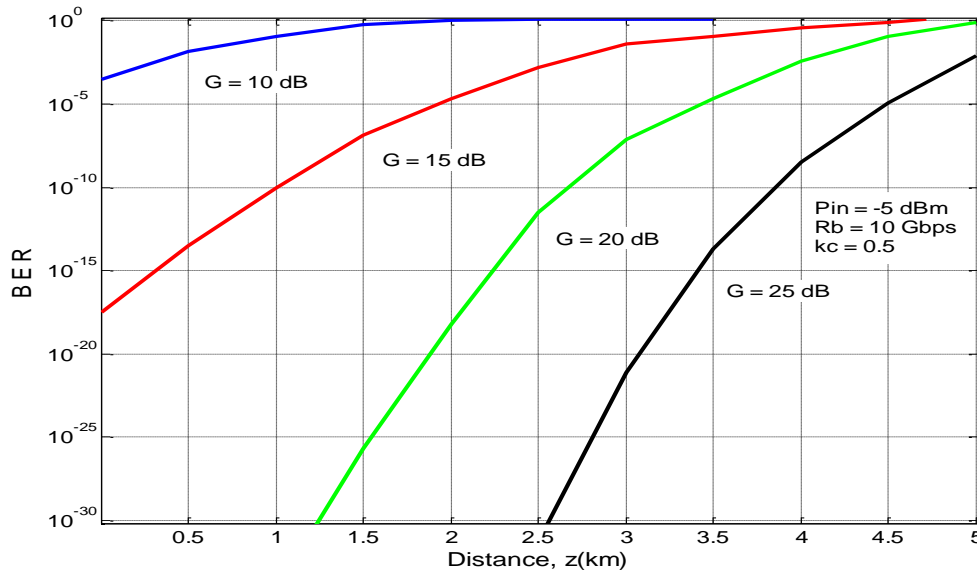


Fig. 3.15 Plots of BER as a function of Transmission distance for different gain (G) level, $R_b = 10$ Gbps, $P_{in} = -5$ dB and $K_c = 0.5$

3.3.8 Effect of Optical Pre-Amplifier Gain on Transmission Distance

In Fig. 3.16, transmission distance is plotted as a function of gain of the optical pre-amplifier. It is seen that transmission distance increases with the increase of gain. Again it is seen that with increase of input power the distance further increases. For example at gain of 15 dB transmission distance covered are 1.5 Km, 2.0 Km and 2.6 Km for - 7 dBm, - 6 dBm and - 5 dBm respectively.

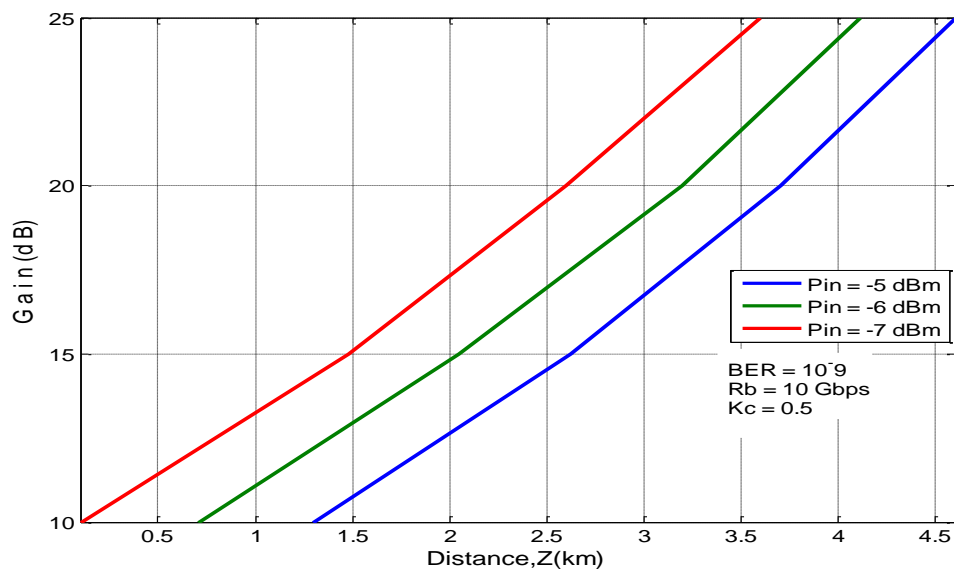


Fig. 3.16 Plots of Transmission Distance as a function of Gain level for different input power, $R_b = 10$ Gbps, $BER = 10^{-9}$ and $K_c = 0.5$

3.3.9 Comparison of Results of with and without Optical Pre-Amplifier

From the comparison of Fig. 3.4© and Fig. 3.12, we find that there is a sharp increase in SCNR due to gain of the optical pre-amplifier at a specific coupling coefficient (say $K_c = 0.5$) even with increased crosstalk and lower power input at Fig. 3.12. For example the SCNR is 31.0 dB (1 Km distance, and power input of -5 dBm) whereas SCNR are 08 dB (1 Km distance, and power input of -3 dBm).

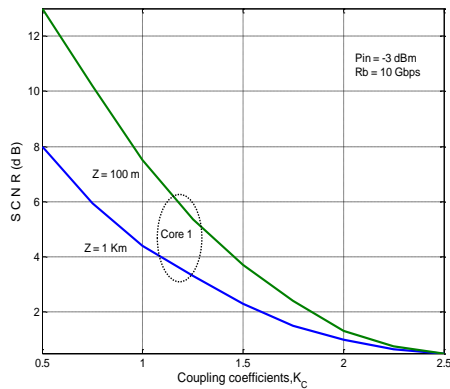


Fig 3.4© Plot of SCNR as a function of K_c without pre-amplifier gain

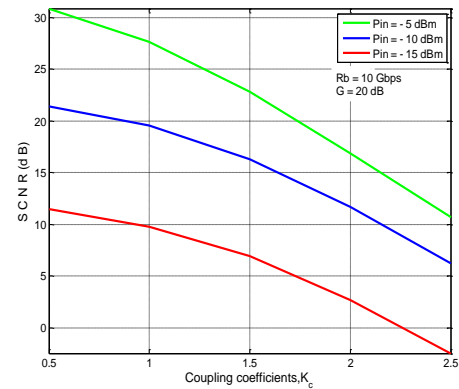


Fig 3.12 Plot of SCNR as a function of K_c with pre-amplifier gain

Again from the comparison of Fig. 3.5(c) and Fig. 3.13, we find that there is significant decrease of BER with the help of pre-amplifier gain at a specific coupling coefficient (say $K_c = 1.0$) even with increased crosstalk and lower power input at Fig. 3.13. For example with pre-amplifier gain and lower input power ($P_{in} = -7$ dBm) BER is 10^{-18} , but the BER is 10^{-5} without gain and input power of, $P_{in} = 1$ dbm.

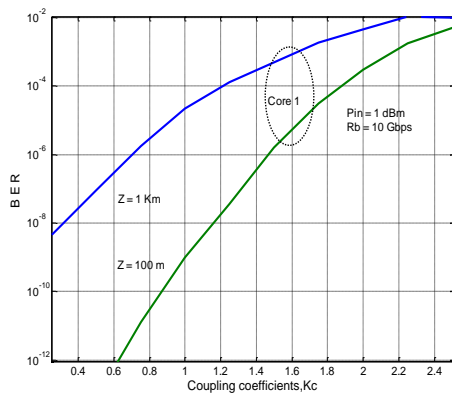


Fig 3.5© Plot of BER as a function of K_c without pre-amplifier gain

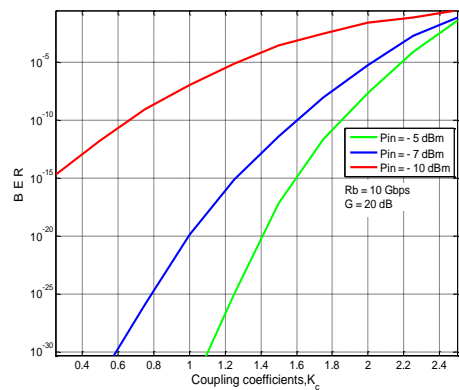


Fig 3.13 Plot of BER as a function of K_c with pre-amplifier gain

CHAPTER 4

CONCLUSION AND SCOPE OF FUTURE WORKS

4.1 Introduction

In this final chapter, we summarize the out-come of our intended research work to fulfill the desired objectives. Here, we also try to provide suggestions for future work.

4.2 Conclusion

In this thesis, we have first theoretically analyzed the effect of crosstalk due to mode coupling in MC-SMF for an optical seven core MCF. An analytical derivation of signal power in desired core and crosstalk power for the same core due to induced power of other cores are carried out. The expression of electrical SCNR and BER is developed due to mode coupling between adjacent cores. The performance of the seven core MCF system is investigated in terms of BER with the variation of input signal power, transmission distance, data rates of input signal and coupling co-efficient etc.

In a seven core MCF communication system, the mode coupling causes the crosstalk and the SCNR is reduced and the BER is increased. With the increase of transmission distance the SCNR decreases. For a fixed coupling co-efficient say $K_c = 0.5$ and varying input data rate the BER increases with the transmission distance, but decreases with the increase of input power. With the increase of coupling co-efficient the BER increases. It is noticed that for a reasonable BER (10^{-9}) the coupling co-efficient has to be reduced with the increase of transmission distance. For higher data rate the coupling co-efficient has to be lowered to attain the same BER of 10^{-9} . It is noticed that to keep the coupling co-efficient constant, the input power in the core has to be increased and with the increase of coupling co-efficient the SCNR decreases. With the increase of data rate, the SCNR decreases. Then the requirement of increase of power due to increase of data rate is found to be necessary, that is to keep the BER at the specified level the input power has to be increased. This increase in power is called power penalty. It is found that for higher coupling co-efficient (K_c) the power penalty are more. It is further noticed that for higher data rate the power penalty is more.

It is noticed that the effect of crosstalk plus the amplifier noises is very significant on the requirement of input power and on the gain of pre-amplifier. When there is no optical pre-amplifier then crosstalk only due to shot noises was considered to evaluate

optical SCR and the input power requirement was -20 dBm to -15 dBm. But when crosstalk along with all beat noises are considered to evaluate the electrical SCNR, then even after the gain of the optical pre amplifier (20 dB) the input power requirement is between -9 dBm to -5 dbm. It is due to the fact that the gain of the pre-amplifier also amplifies the crosstalk also. So, crosstalk plays a vital role in the design of the receiver. Inter core crosstalk due to mode coupling among the adjacent cores is the main reason of quality factor degradation in MCF and it can be mitigated or reduced by proper design of the core to core separation and by applying digital signal processing.

It is marked that both the SCNR and BER decreases with the link distance, but to keep them (SCNR and BER = 10^{-9}) at a fixed level the gain of the pre amplifier should be increased or adjusted. For this system it is seen that to achieve minimum BER of 10^{-9} at least 15 dB gain is required. Again it noticed that, to reach upto desired distance specific gain is required to compensate the crosstalk. For example, to reach a distance of 3.6 km with BER 10^{-9} , at least 25 dB gain is needed.

In [26] F. Y. M. Chan et el. found out a generalized coupling length for the excited core, where as we computed a range of coupling co-efficient of 0.5- 1.7 for allowable data transmission. We also found out the system input power for short distance upto 10 km may be -20 dBm to -15 dBm without gain effect and between -9 dBm to -5 dBm with gain. Finally, we work out to analyze the system model performance at expected value of SCNR and BER for certain optimum parameters. However, considering all the pros and cons, the proposed system explained in this paper not only offers an easy way to evaluate MCF system of short ranges and may be a potential candidate for future MIMO fiber optic communication system.

4.3 Scope of Future Works

Simultaneous excitation in several cores of 7 core MCF will give rise to more crosstalk between the channels. Again for multiple modes in a single core i.e. mode division multiplexing in a single core will increase the crosstalk further. So, future work can include analysis of crosstalk by simultaneous excitation of seven cores and applying MDM in a single core.

The results and expressions may be validated by a simulation work in future

References

- [1] M. Koshiha, K. Saitoh, and Y. Kokubun, "Heterogeneous multi-core Fibers: proposal and design principle," *IEICE Electronics Express*, vol. 6, no. 2, pp. 98-103, Jan. 25, 2009.
- [2] Y. Kokubun and M. Koshiha, "Novel multi-core fibers for mode division multiplexing: proposal and design principle," *IEICE Electronics Express*, vol. 6, no. 8, pp. 522–528, Apr. 25, 2009.
- [3] T. Morioka, Y. Awaji, R. Ryf, P. J. Winzer, D. Richardson, and F. Poletti, "Enhancing optical communications with brand new fibers," *IEEE Commun. Mag.* vol. 50, no. 2, pp. s31– s42, Feb. 9, 2012.
- [4] B.S. Bagad, "Optical Communication", Academy Press, New York, 2009.
- [5] J. M. Senior, "Optical Fiber Communications Principles and Practice, third edition, Prentice Hall International (UK) Ltd, 2009.
- [6] D. K. Maynbaev and L. Scheiner, "Fiber-Optic Communications Technology", Chapter 1, Dorling Kinderley (India) Pvt. Ltd, Pearson Education in South Asia, 2001.
- [7] G. Keiser, "Optical Fiber Communications", Chapter 1, Tata McGraw-Hill, 2008.
- [8] B. Mukherjee, "Optical WDM Networks", Chapter 2, pp. 57-65, Dept of Computer Science, University of California, Davis, CA 95616 USA, 2006.
- [9] G.P. Agrawal, "Fiber Optic communication Systems", Second Edition, New York, John Wiley & Sons, 1997.
- [10] M.S. Kumar, "Fundamentals of Optical Fiber Communication", PHI Learning Pvt. Ltd, Chapter 4, pp. 58-60, 2005.
- [11] Ö. A. Sercan and J. M. Kahn, "Coupled-Core Multi-Core Fibers for Spatial Multiplexing" *IEEE Photonics Technology Letters*, vol. 25, no. 21, Nov. 1, 2013.
- [12] K. Imamura and R. Sugizaki "Recent Advances in Multi-CoreTransmission Fibers" *Proceedings of Opto-Electronics Communications Conference (OECC2012)*, Busan, Korea, July, 2012, pp. 559-560.

- [13] K. Takenga, Y. Arakawa, S. Tanigawa, N. Guan, S. Matsuo, K. Saitoh and M. Koshihara, "Reduction of Crosstalk by Trench-Assisted Multi-Core Fiber" Proceedings of Optical Fiber Communication/National Fiber Optic Engineers Conference, Los Angeles, USA, Mar 2011.
- [14] K. Mukasa, K. Imamura, Y. Tsuchida and R. Sugizaki, "Multi-Core Fibers for Large Capacity SDM" Proceedings of Optical Fiber Communication/National Fiber Optic Engineers Conference, Los Angeles, USA, March 2011.
- [15] D. M. Taylor, C. R. Barnett, T. J. Shepherd, L. F. Michaille, M. D. Nielson and H. R. Simonsen, "Demonstration of Multi-Core Photonic Crystal Fiber in an Optical Interconnect" Electronics Letters, vol. 42, no. 6, pp. 331-332, Mar 2006,.
- [16] M. Koshihara, "Recent Progress in Multi-Core Fibers for Ultralarge Capacity Transmission" Proceedings of Opto Electronics and Communications Conference (OECC2010), Sapporo Convention Center, Japan, pp. 38-39, Jul 2010.
- [17] S. Matsuo, Y. Sasaki, I. Ishida, K. Takenaga, K. Saitoh and M. Koshihara, "Recent Progress on Multi-Core Fiber and Few-Mode Fiber", OFC/NFOEC, 17-23 Mar 2013, Optical Society of America Technical Digest, pp. OM3I.3, Mar 2013.
- [18] J. B. Christos "Advanced Modulation Formats and Multiplexing Techniques for Optical Telecommunication Systems, Trends in Telecommunications Technologies, (Ed.), ISBN: 978-953-307-072-8, InTech, Available from: <http://www.intechopen.com/books>
- [19] J. M. Kahn, K. P. Ho and M. B. Shemirani. "Mode-Coupling Effects in Multimode Fibers", "Optical Fiber Commun. Conf., Los Angeles, CA, USA, March 4-8, 2012".
- [20] R. G. H. van Uden, R. Amezcua Correa, E. Antonio Lopez, F. M. Huijskens, C. Xia, G. Li, A. Schülzgen, H. de Waardt, A. M. J. Koonen & C. M. Okonkwo, "Ultra-high-density spatial division multiplexing with a few-mode multicore fibre" Nature Photonics 8, pp. 865–870, (2014).
- [21] Successful Development of World's First 19-Core Simultaneous Pumped Optical Amplifier. Available from <http://www.nict.go.jp/en/press/2013/10/08-1>
- [22] J. Singh, "Encoding Techniques in Optical CDMA" International Journal of Advanced Engineering Technology, vol. II, issue II, pp. 90-109, April-June, 2011.

- [23] Y. Kokubun, T. Komo, K. Takenaga, S. Tanigawa, and S. Matsuo; “Selective mode excitation and discrimination of four-core homogeneous coupled multi-core fiber.” *Optics Express*, vol. 19, no. 26, Dec 12, 2011.
- [24] A. W. Synder,” *Coupled-mode Theory for optical fiber*,” *J. Opt. Soc. Am.* 62(11), pp. 1267-1277, 1972.
- [25] H. A. Haus and L. Molter-Orr, “Coupled multiple waveguide systems,” *IEEE J. Quantum Electron.* 19(5), pp. 840–844, 1983.
- [26] F.Y.M. Chan, A.P T Lau, and H.Y Tam. “Mode coupling dynamics and communication strategies for multi-core fiber systems”, *Optics Express*, vol. 20, no. 4, Feb 13, 2012.
- [27] M. Abramowitz and I. A. Stegun, “*Handbook of Mathematical Functions*”, (Dover, 1972).
- [28] Fatih Y, Neng Bai, Benyuan Z, Ting W, and Guifang Li; “Long distance transmission in few-mode fibers.”, *Optics Express* , vol. 18, no. 12, June 7, 2010.
- [29] T. Hayashi, T. Taru, O. Shimakawa, T. Sasaki, and E. Sasaoka. “Uncoupled multi-core fiber enhancing signal-to noise ratio.” *Optics Express*, vol. 20, no. 26, Dec 2012.
- [30] S. M. Jahangir Alam, M. Rabiul Alam, Guoqing Hu, and Md. Zakirul Mehrab, “Bit Error Rate Optimization in Fiber Optic Communications” ; *International Journal of Machine Learning and Computing*, vol. 1, no. 5, Dec 2011.